Cerebral Cortex May 2015;25:1362–1378
doi:10.1093/cercor/bht328
Advance Access publication December 8, 2013

Auditory Responses and Stimulus-Specific Adaptation in Rat Auditory Cortex are Preserved Across NREM and REM Sleep

Yuval Nir[1,2], Vladyslav V. Vyazovskiy[1,3], Chiara Cirelli[1], Matthew I. Banks[4] and Giulio Tononi[1]

[1]Department of Psychiatry, University of Wisconsin-Madison, Madison, WI 53719, USA, [2]Department of Physiology and Pharmacology, Sackler School of Medicine, and Sagol School of Neuroscience, Tel Aviv University, Tel Aviv 69978, Israel, [3]Department of Physiology, Anatomy and Genetics, University of Oxford, Oxford OX1 3QX, UK and [4]Department of Anesthesiology, University of Wisconsin, Madison, WI 53706, USA

Address correspondence to Dr Yuval Nir, Department of Physiology and Pharmacology, Sackler School of Medicine, and Sagol School of Neuroscience, Tel Aviv 69978, Israel. Email: ynir@post.tau.ac.il

Sleep entails a disconnection from the external environment. By and large, sensory stimuli do not trigger behavioral responses and are not consciously perceived as they usually are in wakefulness. Traditionally, sleep disconnection was ascribed to a thalamic "gate," which would prevent signal propagation along ascending sensory pathways to primary cortical areas. Here, we compared single-unit and LFP responses in core auditory cortex as freely moving rats spontaneously switched between wakefulness and sleep states. Despite robust differences in baseline neuronal activity, both the selectivity and the magnitude of auditory-evoked responses were comparable across wakefulness, Nonrapid eye movement (NREM) and rapid eye movement (REM) sleep (pairwise differences <8% between states). The processing of deviant tones was also compared in sleep and wakefulness using an oddball paradigm. Robust stimulus-specific adaptation (SSA) was observed following the onset of repetitive tones, and the strength of SSA effects (13–20%) was comparable across vigilance states. Thus, responses in core auditory cortex are preserved across sleep states, suggesting that evoked activity in primary sensory cortices is driven by external physical stimuli with little modulation by vigilance state. We suggest that sensory disconnection during sleep occurs at a stage later than primary sensory areas.

Keywords: auditory cortex, NREM sleep, oddball, rat, REM sleep, single unit

Introduction

A defining feature of sleep is that it brings about a reversible reduction in behavioral responsiveness. Such a high "arousal threshold" is evident in NREM sleep and persists also in REM sleep (Rechtschaffen et al. 1966; Neckelmann and Ursin 1993). Accordingly, external stimuli fail to elicit an adequate behavioral response unless they are strong enough to cause an awakening, as may happen with the sound of an alarm clock. Moreover, stimuli largely fail to be incorporated in the content of dreams (Rechtschaffen 1978; Nir and Tononi 2010). For example, if we are to sleep all night in front of the television, our dreams will have little, if anything, to do with the contents of the surrounding stream of sounds. During anesthesia and NREM sleep, sensory processing may be expected to be different than during wakefulness, since the thalamocortical system is active in a drastically different mode with hyperpolarized cortical neurons alternating between active and silent periods (Steriade et al. 2001). However, a high arousal threshold persists during REM sleep when the thalamocortical system is depolarized with a wake-like "activated" low-voltage electroencephalogram (EEG), and when neurons fire tonically much like during wakefulness (Steriade et al. 2001). Therefore, disconnection continues throughout sleep and its diverse modes of activity and poses an unsolved paradox.

Despite the disconnection from the external environment during sleep, it is also clear that some sensory processing and discriminative capacity persists. For example, sleeping humans may respond more readily to their name being called when compared with other names and sounds (Oswald et al. 1960; McDonald et al. 1975) and evoked potentials triggered by semantically incongruous words may be elicited in some stages of human sleep (Bastuji et al. 2002). Given the disconnection on one hand, and the residual processing on the other, it remains unclear to what extent the signal propagation along ascending sensory pathways that occurs during wakefulness is preserved during sleep. Compared with the large body of literature in acute anesthetized preparations, only very few studies examined sensory responses at the neuronal level during natural sleep [see Hennevin et al. (2007) for review].

Owing to its burst-silence mode of activity during NREM sleep, the thalamus has been traditionally considered as the major processing node where sensory signal transmission is attenuated during sleep. Accordingly, sleep disconnection may be due to "thalamic gating" where peripheral sensory inputs are not relayed effectively to the cortex (McCormick and Bal 1994; Steriade 2003). Along this line, attenuated single-unit responses in thalamic sensory relay nuclei have been observed during NREM sleep in primates, cats, and rodents (Mukhametov and Rizzolatti 1970; Livingstone and Hubel 1981; Mariotti et al. 1989; Edeline et al. 2001). In addition, studies of primary visual (Evarts 1963; Livingstone and Hubel 1981) and somatosensory (Gucer 1979) cortices demonstrated attenuated responses in sleep, but large variability exists between studies and between cortical cells.

In the auditory system, it remains particularly undecided to what extent primary auditory cortex (PAC) responds to sounds during sleep (PAC is used throughout this article to refer to core auditory fields receiving input from the ventral division of the medial geniculate nucleus of the thalamus). Early evoked potential studies in the rat found enhanced responses during NREM sleep and comparable responses in REM sleep (Hall and Borbely 1970). Early single-unit studies in cats and primates suggested that PAC responses were weaker in sleep compared with wakefulness (Murata and Kameda 1963; Brugge and Merzenich 1973) but recent single-unit studies in guinea pigs and primates found comparable responses (Pena et al. 1999; Edeline et al. 2001; Issa and Wang 2008) apart from potential subtle differences (Issa and Wang 2011). Functional imaging in humans has also yielded mixed results; some studies argue for comparable activation in sleep and wakefulness at the level of

PAC (Portas et al. 2000) whereas others argue for decreased activity in sleep (Czisch et al. 2002).

Apart from basic processing of sounds in PAC (e.g., selectivity to acoustic features, response magnitude) which could be preserved during sleep (Pena et al. 1999; Edeline et al. 2001; Issa and Wang 2008), the degree to which context-dependent processing is maintained in sleep remains unknown. In humans, infrequent stimuli in a sequence of sounds elicits, in awake subjects, a midlatency (150–250 ms) characteristic EEG event-related potential (ERP) called the mismatch negativity (MMN) followed by a late (>250 ms) P300/P3 wave (Naatanen et al. 2011). In general, the MMN reflects preattentive processing whereas the P3 is correlated with perceptual awareness (Dehaene and Changeux 2011). Evoked potential studies in sleeping humans found evidence for differential responses to oddball stimuli in some circumstances (Niiyama et al. 1994; Perrin et al. 1999, 2000; Ruby et al. 2008), but the magnitude and spatial extent of the P3 may be reduced (Cote 2002; Colrain and Campbell 2007). Animal studies have also used auditory oddball paradigms to examine, at the neuronal level, both early and late components in the responses to frequent and infrequent stimuli. Studies of early responses typically focus on stimulus-specific adaptation (SSA) of single neurons in the auditory thalamus and cortex. SSA has been extensively studied in anesthetized cats and rodents, and is believed to represent the cellular information processing that eventually gives rise to the MMN (Nelken and Ulanovsky 2007). Along this line, deviance sensitivity observed in human midlatency potentials suggests that SSA is present in human auditory cortex (Costa-Faidella et al. 2011). Other studies reported that infrequent deviant tones could also trigger long-latency (>200 ms) ERPs, particularly, when rare tones were associated with rewards or aversive outcomes through training (Yamaguchi et al. 1993; Shinba 1997). However, the processing of deviant sounds at the neuronal level during natural sleep remains unknown.

In the present study, we compared single-unit and local field potential (LFP) responses as well as SSA in PAC of rats across wakefulness and natural sleep. The aims of this study were 3-fold: 1) to examine the degree to which responses in PAC are preserved during sleep in rodents, the most common model system for studying sleep and sleep regulation, and one that is most suitable for future studies in transgenic animals when employing novel tools such as calcium imaging and optogenetics; 2) to check whether comparable PAC responses are preserved also in unrestrained animals as they undergo natural physiological sleep. All previous studies of single-unit auditory responses in sleep were conducted in restrained animals to achieve maximal control over acoustic stimulation. However, such conditions may not be favorable for neither alert wakefulness (locomotion may have dramatic effects on activity in primary sensory cortices (Keller et al. 2012)) or deep sleep (associated with marked reduction in baseline firing rates and neuronal bistability), thereby limiting the potential contrast between these vigilance states, 3) to examine to what degree differential responses to deviant stimuli (e.g., SSA) are maintained in single-unit responses during sleep.

Materials and Methods

Subjects and Surgery

Adult male WKY rats ($n = 6$, 300–350 g, Harlan Ltd.) were housed individually in transparent Plexiglas cages. Lighting and temperature were kept constant (LD 12:12, light on at 10:00 AM, 23 ± 1 °C; food and water available ad libitum). All procedures related to animal handling, recording, and surgery followed the NIH Guide for the Care and Use of Laboratory Animals, and were approved by the Institutional Animal Care and Use Committee (IACUC). Three days prior to surgery, rats were placed in their home cage within the acoustic chamber for habituation to the experimental environment. One day before surgery animals received an i.p. dose of dexamethasone (0.2 mg/kg) to suppress local immunological response and reduce edema (Vyazovskiy, Olcese et al. 2011).

Under deep isoflurane anesthesia (1.5–2% volume), microwire arrays were implanted targeting the right PAC in 6 animals (centered at B: −4.3 mm, L: +6.7 mm, D: −4.6 mm) and in 3 animals also in the right frontal cortex (centered at B: +2 mm, L: +2 mm, D: −2 mm; Fig. 1*A–C*). The arrays consisted of 16-channel (2 rows of 8 wires each), 33-µm polyimide-insulated tungsten microwires (Tucker-Davis Technologies, Inc. (TDT), Alachua, FL, USA; spacing between microwires: 175–250 µm; separation between rows: L–R: 375–500 µm, D–V: 0.5 mm). Surgery was performed in sterile conditions, using Ethylene oxide sterilized materials, following procedures described in Kralik et al. (2001) and Vyazovskiy, Olcese et al. (2011). Under microscopic control, a ~2 × 2-mm craniotomy was made using high-speed surgical drills. The dura was carefully dissected and electrode arrays were advanced into the brain tissue by penetrating the pia mater while carefully avoiding vasculature. Two-component silicone gel (KwikSil; World Precision Instruments, FL, USA) was applied to seal the craniotomy and protect the brain surface. After gel polymerization, dental acrylic was gently placed around the electrode, fixing the array to the skull. EEG screws were placed over the left frontal and parietal cortices. Ground and reference screw electrodes were placed above the cerebellum, and neck muscle electrodes were implanted for electromyography (EMG).

Electrophysiology

We continuously recorded concurrently extracellular spike data (filtered 300–5000 Hz), LFPs from the same microelectrodes (filtered 0.1–100 Hz), epidural EEGs (filtered 0.1–100 Hz), muscle tone via EMG (filtered 10–100 Hz) using a TDT PZ amplifier and RZ2 acquisition system, as well as synchronized continuous infrared video recordings (OptiView Technologies, Inc.), as in Vyazovskiy, Olcese et al. (2011).

Amplitude thresholds for online spike detection were set manually upon careful visual inspection (OpenEx software, TDT). In all cases, thresholds exceeded −25 µV and ensured a SNR >2 (see Supplementary Fig. 1 for examples). Whenever the recorded voltage in the high-pass filtered signal (>300 Hz) exceeded this threshold, a segment of 46 samples (1.84 ms) was extracted together with corresponding time-stamps and stored for subsequent analysis. We refer to the resulting binary signal with putative action potentials (prior to spike sorting) as multiunit activity (MUA) throughout the article. Spike sorting was performed offline by superparamagnetic clustering of wavelet coefficients (Quian Quiroga et al. 2004), and complemented by visual inspection of action potential waveforms, their variability, and interspike-interval (ISI) distributions. Based on the consistency of waveforms and the occurrence of ISIs within the expected refractory period (<3 ms), we categorized clusters as either mixed clusters, single-unit clusters, or noise clusters (the latter were not analyzed).

Scoring Vigilance States and Behavioral Analysis

Vigilance states were manually scored in 4-s epochs based on visual inspection. SleepSign software (Kissei) was used to simultaneously visualize offline EEG, LFP, EMG, and behavior (video). Wakefulness was defined as epochs dominated by low-voltage, high-frequency EEG/LFP patterns and phasic EMG activity. Epochs of eating, drinking, and intense grooming (<5%) were excluded to minimize artifacts. NREM sleep was defined as epochs with high-amplitude slow waves and low tonic EMG activity. REM sleep was defined as epochs where the EEG/LFP was similar to that during waking with slightly more pronounced theta rhythms in posterior derivations, while the EMG contained solely heartbeats and occasional twitches. Mixed epochs (10.5%, including transitions and artifacts) were categorized separately

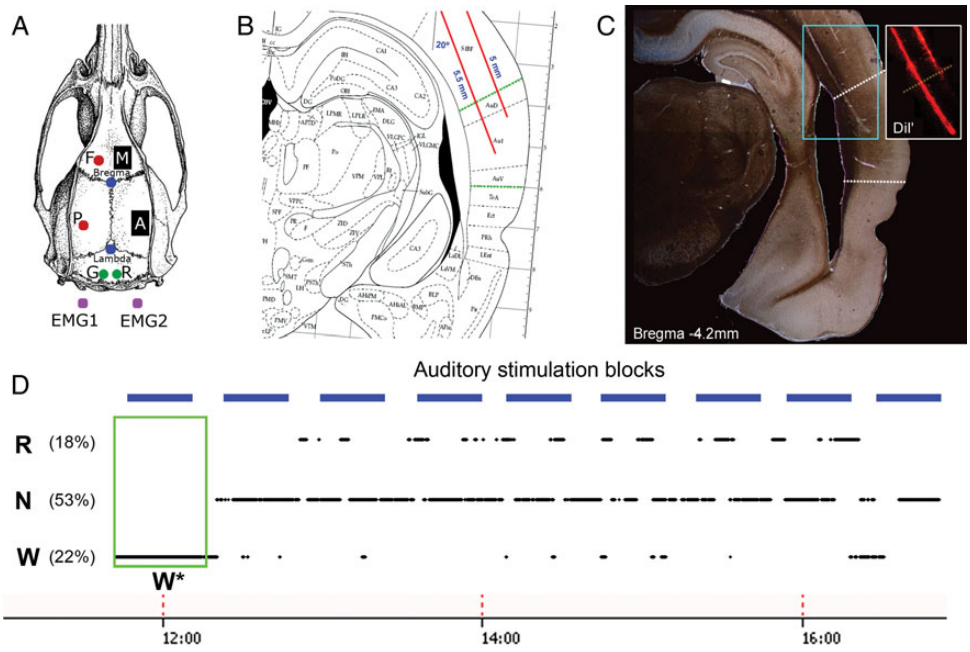

Figure 1. Experimental setup. (*A*) Recording arrangement included a 16-microwire array implanted in the right auditory cortex ("A", $n = 6$), a control 16-microwire array placed in the right motor cortex ("M", $n = 3$), EEGs from frontal "F" and parietal "P" derivations (red circles), ground "G" and reference "R" screws placed over the cerebellum (green circles), and bilateral neck muscle electrodes for electromyography (EMG). (*B*) Sketch of surgical plan with oblique implantation of auditory microwires (red lines) superimposed with a coronal diagram of the rat brain 4.5 mm posterior to Bregma (Paxinos and Watson 1986); dotted green lines denote borders of auditory cortex. (*C*) Representative histological verification of location of electrodes coated with DiI fluorescent dye (Materials and Methods); dotted white lines denote putative borders of primary auditory cortex. Inset shows fluorescence image corresponding to cyan area. (*D*) Example auditory stimulation protocol superimposed with changes in vigilance states. Sessions started around noon (time on bottom) and lasted 3–5 h. Experiments included repeated identical blocks of sound stimulation (horizontal blue bars, top), interleaved with 10-min silent intervals. Rats were kept continuously awake during the first block of stimulation (green box, W*) and were left undisturbed during all other blocks. W, N, and R correspond to wakefulness, NREM sleep, and REM sleep, respectively. Note that percent time spent in each vigilance state does not add to 100% since mixed epochs were not further analyzed (Materials and Methods).

and excluded from further analysis. Joint distributions of EMG levels and high-/low-frequency energy ratio in the EEG (as in Fig. 2*D*) were computed for each session separately to further verify proper separation to vigilance states. The high-/low-frequency energy ratio was computed using 25–100 and 1–4 Hz frequency bands, respectively.

Phasic EMG events reflecting a muscle twitch and/or startle response evoked by a minority (<5%, see Results) of high-intensity (80 dB SPL) sounds were automatically detected in Matlab (The MathWorks, Natick, MA, USA). To this end, the instantaneous amplitude of the EMG signal was extracted via the Hilbert transform and smoothed with a Gaussian kernel ($\sigma = 10$ ms). Events with amplitude above 3.5 SD occurring within the first 75 ms following sound onset were identified. These parameters were optimized after careful comparison of automatically detected events with behavioral video recordings to minimize misses and false positives.

Acoustic Setup and Auditory Stimuli

All experiments were conducted in a foam-insulated cage placed within a double-wall soundproof chamber (Industrial Acoustics Company, Bronx, NY, USA). Sounds were synthesized online using Matlab, transduced to voltage signals by a high-sampling rate (192 kHz) sound card (HDSP9632, RME, Germany), amplified (SA1, TDT), and played free-field through a magnetic speaker (MF1, TDT) mounted 35 cm above the animal. All sounds were stereo signals where one channel (containing the sound of interest) was routed to the mono speaker, whereas the other channel (containing a brief synchronization pulse) was routed to the electrophysiology acquisition system. Acoustic calibration was performed in situ with a calibrated condenser microphone placed on the cage's floor 35 cm below the speaker (#4016, ACO Pacific, Inc., Belmont, CA, USA). Intensity levels for frequencies in the range of 1–64 kHz were measured, attenuation factors were computed (all below 10 dB across frequencies), and then applied to the original stimuli to reach a flat output (± few dB) independently for output levels of 30, 55, and 80 dB SPL. Actual levels varied on each trial given that stimuli were free-field and animals were not restrained.

The stimulus set consisted of 24 simple and complex sounds, including 9 short (100 ms) pure tones (256 Hz to 64 KHz with octave spacing; 5-ms onset/offset linear ramps); 3 long (600 ms) pure tones (4, 8, and 16 kHz; 5-ms onset/offset linear ramps); 1 click; 1 click train (interclick interval = 20 ms, duration = 500 ms); 3 environmental ecologically relevant sounds recorded at the laboratory (cage door opening and closing, room door opening and closing, and experimenter's voice, durations = 800 ms); 3 rat vocalizations (Avisoft Bioacoustics, Germany) with carrier frequencies of 22, 40, and 60 kHz and durations 250–1000 ms; 2 "chirp-modulated" AM sounds (carrier frequency = 10 kHz, f(mod) = 20–200 Hz or 200–20 Hz, duration = 600 ms) as in Artieda et al. (2004); and 2 frequency modulation (FM) sweeps (0.5–2 or 2–0.5 kHz, duration = 100 ms). All sounds were digitally designed to occupy 95% of the maximal dynamic range of the soundcard (voltage) to avoid clipping, and subject to further amplification to reach final outputs of 30, 55, and 80 dB SPL (see above).

Experimental Design

One week was allowed for recovery after surgery, and experiments started only after the sleep/waking cycle had normalized, as evidenced by the entrainment of sleep and wake by the light/dark cycle and the homeostatic time-course of slow-wave activity (power <4 Hz) in sleep (Vyazovskiy, Cirelli et al. 2011). Prior to experiments, rats were well habituated to the experimenter and to exposure of novel objects (exposure to new objects every day at light onset for 30 min/day). In addition, 5 days following surgery, we started to gradually expose the animals to acoustic stimuli (session length and intensity levels were incremented daily) until animals adapted and were able to comfortably maintain consolidated sleep while sounds were played (no observable muscle twitches for sounds at 30 and 55 dB SPL, and <10% of 80 dB SPL trials associated with muscle twitches).

Experimental sessions started around noon (animals were allowed to sleep uninterrupted for 2 h starting at lights-on at 10:00 AM) and lasted 3–5 h. This timing was chosen in order to maximize the chances that sufficient trials during REM sleep will be available for subsequent

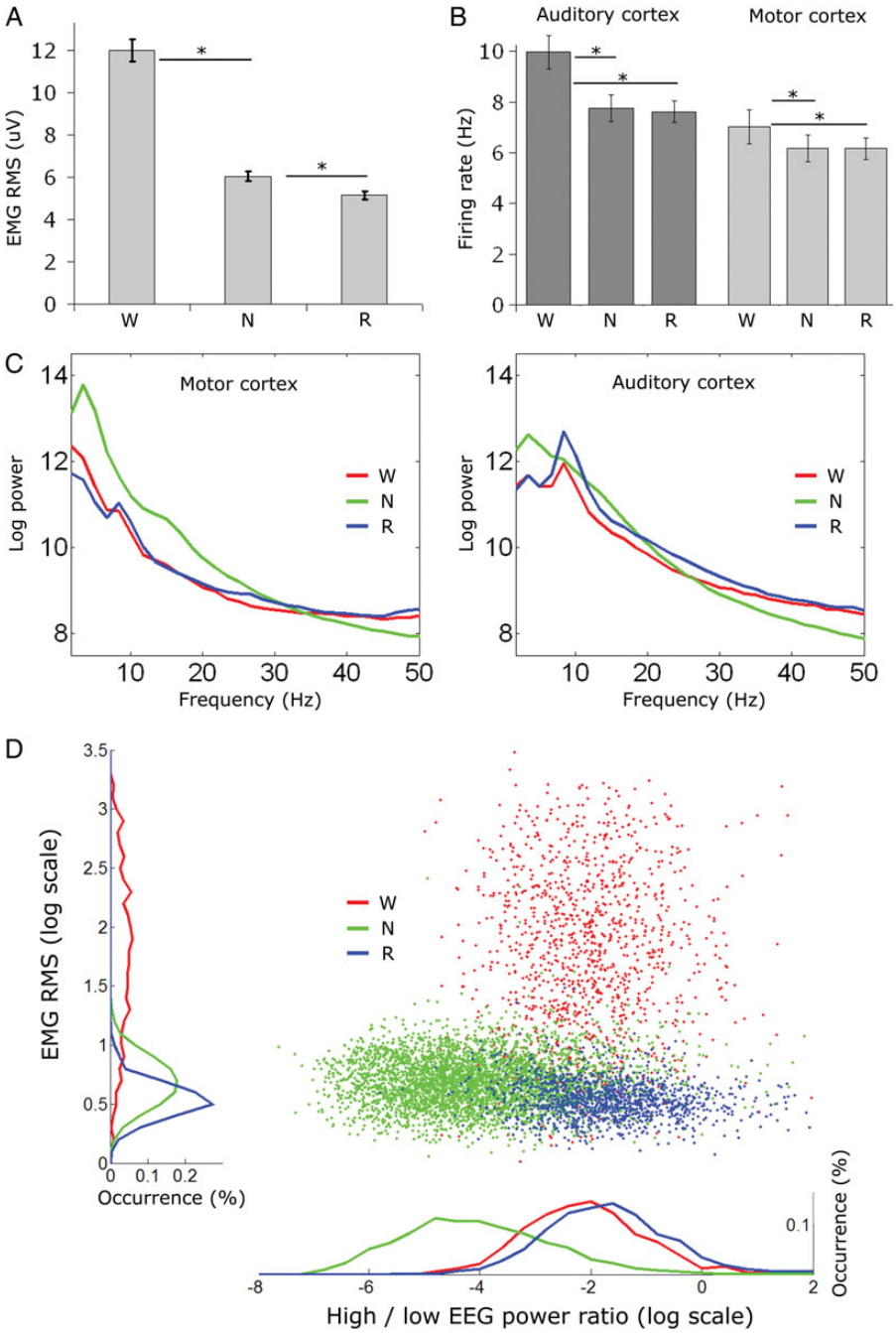

Figure 2. Prestimulus baseline activity differs across vigilance states. (*A*) EMG dynamic range across vigilance states ($n = 10$ sessions); muscle tone is highest during wakefulness, lower in NREM sleep, and minimal in REM sleep; all asterisks mark statistical significance of at least $P < 10E\text{-}7$ (paired *t*-tests). (*B*) Baseline neuronal firing rates. Firing rates in auditory cortex (PAC, $n = 295$) as well as motor cortex (M1, $n = 94$) are higher in wakefulness than in NREM and REM sleep. Asterisks as in A (*C*) LFP power spectra in motor cortex (left, $n = 80$ channels) and auditory cortex (right, $n = 160$ channels) across vigilance states. Note that slow-wave activity (power < 4 Hz) is maximal in NREM sleep (green), particularly in the frontal lobe, while high-frequency (>30 Hz) power is maximal in wakefulness (red) and REM sleep (blue). In addition, theta (5–9 Hz) power is higher in wakefulness and maximal in REM sleep, particularly in the auditory cortex. (*D*) Joint distribution of EMG levels and high-/low-frequency energy ratio in the EEG in a representative session. Colors as above. Note that both NREM and REM sleep are characterized by low EMG levels, whereas REM sleep and wakefulness are characterized by a dominance of high-frequency power in the EEG.

analysis. Each experiment consisted of repeated identical blocks of sound stimulation (Fig. 1*D*; details below), interleaved with 10-min intervals with no stimulation. During the first block of stimulation in each session, rats were kept continuously awake by providing them with novel objects (Vyazovskiy, Olcese et al. 2011), in order to allow for separate subsequent analysis of auditory responses during consolidated wake periods (W*). In all other stimulation blocks, animals were left undisturbed. Two different experiments (main, oddball) were run on separate days as given below.

Main Experiment

In each 30-min block, all 24 sounds were presented at 3 intensity levels (30/55/80 dB SPL) each for a total of 72 different stimuli. Each stimulus was presented 15 times (a total of 1080 trials per block) in a pseudorandom order with interstimulus intervals (ISIs, offset to onset) of 1250 ± 250 ms.

Oddball Experiment

Each 13.5-min block included 2 parts; in Part A, an 8-kHz tone was presented frequently ($n = 450$, 90%), whereas a 45-kHz tone was

presented rarely ($n = 50$, 10%). Both tones were 100 ms in duration with 5-ms onset/offset linear ramps. In Part B, tones were swapped such that the 8-kHz tone was "standard" and the 45-kHz tone was "deviant." Both tones were presented at 55 dB SPL in a pseudorandom order with ISIs of 750 ± 100 ms.

Histology

Upon completion of the experiments, the position of electrodes was verified by histology in all animals. Animals were perfused with 4% paraformaldehyde/PBS under deep isoflurane anesthesia (3% in oxygen), brains were postfixed, rapidly frozen on dry ice, cut into 50-µm serial coronal sections, and subjected to Cresyl Violet (Nissl) staining. Histological verification confirmed that electrodes were located within areas Au1/AuV/AuD as defined by (Paxinos and Watson 1986) and a recent study supporting a slightly extended dorsal border (Doron et al. 2002). The most recent physiological studies in the rat indicate that these anatomical regions are where tonotopically organized core (primary) auditory fields are located (Polley et al. 2007). In 2 of 6 animals, microwire arrays were coated 1 day prior to surgery with a thin layer of DiI fluorescent dye (DiIC18(3), Invitrogen) under microscopic control to facilitate subsequent localization (Magill et al. 2006), as seen in Figure 1*C*.

Data Analysis

Analysis of Auditory Responses

All data analyses were carried out offline with Matlab. Evoked LFP and MUA responses (Fig. 3) focused on tone pips (27 of 72 of all stimuli) whose duration was identical (100 ms). Comparison of MUA onset responses across stimulus intensities and vigilance states was performed using a two-way ANOVA using the maximal peak of the response in the interval 10–30 ms after stimulus onset. For isolated SUA recordings, significant changes in firing rate in time intervals corresponding to onset, offset, and sustained periods were detected as follows. First, spike trains were aligned on stimulus onset, averaged across trials, and binned (bin size = 25 ms). Onset and offset intervals were defined as the first 25 ms bin following sound onset and offset, respectively. Sustained intervals were defined as all other bins during stimulus presentation. Changes in firing rate were detected in the interval of interest (onset/offset/sustained) by comparison with prestimulus baseline periods (600 ms prior to stimulus onset) in a particular state via Student's *t*-tests. Given that we conducted multiple *t*-tests (in the main experiment, 389 units × 72 stimuli × checking for increases/decreases in onset/offset/sustained intervals resulted in 473 428 tests), we corrected for multiple comparisons using false discovery rate (FDR) control for familywise error (Benjamini and Yekutieli 2001). FDR was controlled such that $q(\text{FDR}) < 0.05$ for each state separately (corresponding to critical *P*-values in the range 0.0036–0.006), thereby achieving the same statistical strength across vigilance states and utilizing all available data, despite having a different number of trials in each state. Similar results were obtained when selecting the same number of trials in each state for analysis. In general, our simple algorithm performed well across different conditions, agreeing with visual inspection of responses, and was robust to the precise choice of threshold (e.g., $P < 0.01$ or $P < 0.0001$ uncorrected) and bin size (15, 25, 50, and 100 ms) such that these parameters did not affect the main results reported.

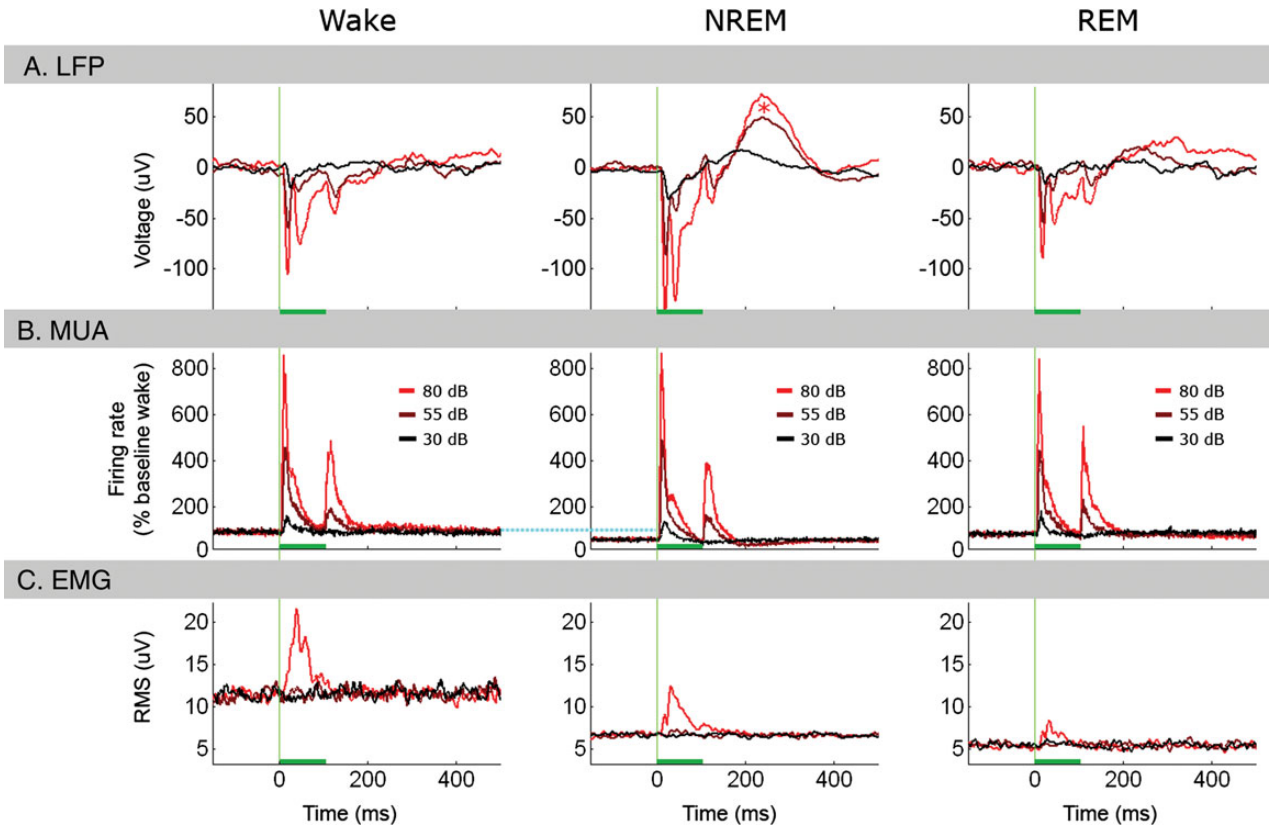

Figure 3. Overview of evoked responses in main experiment. Overview of evoked responses to 100-ms tones across vigilance states ($n = 10$ sessions in 6 animals). (*A*) Average event-related LFP responses recorded in auditory cortex ($n = 160$ channels, $N = 2333$, 4957, and 1458 tones in Wake, NREM, and REM sleep, respectively) in response to low (30 dB, black), medium (55 dB, brown), and high-intensity (80 dB, red) tones. Horizontal green bars mark stimulus duration. Vertical green lines mark tone onset. Note that LFP responses are nearly identical in wakefulness and REM sleep, whereas, in NREM sleep, they are larger in amplitude and followed by a positive peak (red asterisk) corresponding to a poststimulus suppression of neuronal activity. (*B*) Evoked multiunit activity from the same channels in auditory cortex in response to tones; colors and intensities as above. Note that both onset and offset MUA responses are parametrically related to stimulus intensity and highly similar across vigilance states, despite difference in baseline firing rates (horizontal dotted cyan line). (*C*) EMG evoked by auditory stimuli reveals that high-intensity (80 dB) tones elicit detectable transient changes in muscle tone corresponding to a startle response, whereas low- and medium-intensity stimuli do not elicit any changes above baseline. In addition, differences in prestimulus baseline values replicate those in Figure 2.

Analysis of Latency of Excitatory Onset Responses

For each auditory unit for which an excitatory onset response was detected for at least 1 stimulus ($n = 195/295$ units, see above), a peristimulus time histogram (PSTH) was created for each stimulus separately (without binning) in a window beginning 600 ms before stimulus onset and terminating 600 ms poststimulus onset. For each onset response, onset latency was defined as in Polley et al. (2007), as the intersection between the slope of the excitatory response profile and the mean prestimulus firing rate (illustrated in Fig. 5*B*). Finally, the onset latency of each neuron was defined as the average onset latency across all stimuli that elicited onset responses for that neuron (latencies did not significantly differ across intensities).

Comparison Across Vigilance States

Once every condition (stimulus) in every state (wake/sleep) was tagged for the presence of various responses (i.e., changes in firing rate), we proceeded to compare quantitatively the selectivity and response magnitude across states. Selectivity was defined in this context as the percent of suprathreshold stimuli (excluding 30SPL) for which responses were detected, and response magnitudes were computed using the mean discharge rate (spikes per second). Modulation gain factors (Fig. 7, bottom) were extracted for each pair of vigilance states in each recording session separately according to the following formula, as in Issa and Wang (2008):

$$\%\mathrm{Gain}_{i-j} = \frac{R_i - R_j}{\max(|R_i|, |R_j|)},$$

where R_i and R_j are the discharge rates during vigilance states i and j, respectively. Gains were computed for each stimulus separately. Conclusions were unaffected when expressing response magnitudes in firing rates normalized by the baseline firing rate in each vigilance states, instead of absolute spikes per second. For each pairwise comparison between states (e.g., NREM versus wake), we checked whether the mean gain factor represented a significant deviation from a null (zero-centered) distribution using bootstrapping as follows. For each stimulus separately, we assigned a random vigilance state label instead of the real one, and otherwise computed the mean gain value across the entire dataset using the exact same procedure as for the real data. This procedure was repeated across 10 000 iterations to create the null distribution of average gain values. The *P*-value associated with each real pairwise comparison was computed by examining the percent of random iterations that showed an average gain equal or greater than the one observed in real data.

We also computed modulation gain factors between each pair of vigilance states for each unit (collapsed across stimuli with significant responses). For each pair of vigilance states and for each neuron separately, a two-tail Student *t*-test ($P < 0.05$) was used to determine, if that unit was significantly modulated in either direction. The overall conclusions were not affected by whether gain factors were computed per stimulus or per neuron, given that the majority of units did not show significant modulations (see Results).

Analysis of Stimulus-specific Adaptation Effects

Data from oddball experiments were analyzed as follows. Analysis was limited only to cases in which both frequencies evoked significant responses in at least the "deviant" condition to avoid cases in which neuronal activity was not driven by both frequencies. The strength of the LFP onset response was quantified by the depth of the maximal negative trough of the average response in the interval 10–30 ms after stimulus onset. Similarly, MUA onset responses were quantified by the maximal positive peak of the average response in the interval 10–30 ms after stimulus onset. To obtain estimates of instantaneous SUA firing rate modulations (in order to quantify those in a comparable manner to LFP and MUA signals above), spike trains were aligned on stimulus onset, averaged across trials, and smoothed with a Gaussian kernel ($\sigma = 5$ ms). The strength of SUA responses in the oddball paradigm was then quantified as the increase in firing (maximal positive peak in the interval 10–30 ms after stimulus onset minus the baseline firing rate). To quantify, for each frequency separately, the effect of presentation probability (SSA), we calculated the contrast between the responses to that frequency f_i when it was standard and when it was deviant (Fig. 9*A*), called the "SSA index" or SI_i:

$$\mathrm{SI}_i = \frac{d(f_i) - s(f_i)}{d(f_i) + s(f_i)},$$

where $d(f_i)$ and $s(f_i)$ represent the peak responses to frequency f_i when it was deviant and standard, respectively (Ulanovsky et al. 2003; Taaseh et al. 2011). In addition, the average SSA effect between deviant and standard responses across both frequencies (Fig. 9*B*) was further defined as the common SSA index (CSI):

$$\mathrm{CSI} = \frac{d(f_1) + d(f_2) - s(f_1) - s(f_2)}{d(f_1) + d(f_2) + s(f_1) + s(f_2)}$$

Results

Adult WKY rats were implanted with microwire arrays targeting the PAC ($n = 6$) and the motor cortex ($n = 3$) in the right hemisphere (Fig. 1). Histological verification confirmed that arrays were indeed located within core auditory cortex (Fig. 1*C*). After a week of recovery, sleep stabilization, and habituation to stimulation, acoustic stimuli were presented as animals spontaneously switched between vigilance states (Supplementary Fig. 2). In the main experiment ($n = 10$ sessions), responses to a wide battery of stimuli included tones, clicks and click-trains, complex environmental sounds, rat vocalizations, FM sweeps, and "chirp AM" tones. LFPs and SUA ($n = 389$) were recorded continuously along with epidural EEG, EMG, and video (see Materials and Methods for additional information).

Prestimulus Baseline Activity Differs Across Vigilance States

Vigilance states were scored in 4-s epochs on the basis of EEG, LFP, EMG, and behavior, and each trial of sound presentation was categorized as occurring during wakefulness (23.8 ± 2.2%), NREM sleep (50.6 ± 1.5%), REM sleep (15.1 ± 1.6%), or mixed epochs (10.5 ± 1.9%) which were not further analyzed. The average duration of vigilance states was 70 s for wakefulness (±6.9 s, median = 28 s, range: 4–1584 s), 87 s for NREM sleep (±2.9 s, median = 56 s, range: 4–928 s), and 72 s for REM sleep (±3.8 s, median = 40 s, range: 4–416 s). We first compared the baseline activity in prestimulus intervals. As expected, muscle tone was highest during wakefulness (mean RMS 12.0 ± 0.5 μV), lower in NREM sleep (6.0 ± 0.2 μV), lowest during REM sleep (5.2 ± 0.2 μV, Fig. 2*A*), and these differences were highly significant statistically (one-way analysis of variance (ANOVA) on mean RMS values; $P < 8.29\mathrm{E}{-42}$, $F > 106$ for vigilance state). Spontaneous neuronal firing rates were lower in sleep compared with wakefulness (Fig. 2*B*). For example, in PAC ($n = 295$) firing in NREM and REM sleep was 79.9 ± 1.6% and 77.4 ± 2.1% of that in wakefulness, respectively ($P < 0.0005$, $F > 7.8$ via ANOVA for vigilance states). Firing rates in motor cortex during NREM sleep ($n = 94$) were likewise lower than those in wakefulness ($P < 10\mathrm{E}{-7}$ via paired *t*-test). Furthermore, power spectra of prestimulus baseline LFP signals (Fig. 2*C*) showed many well-established properties of vigilance states. Slow-wave activity (EEG spectral power below 4 Hz) was maximal in NREM sleep, particularly in the frontal lobe, while high-frequency (>30 Hz) power was maximal in wakefulness and REM sleep. In addition, theta (5–9 Hz) power was higher in wakefulness and maximal in REM sleep, particularly

in the auditory cortex, probably due to its proximity to the hippocampus. Joint distributions of EMG levels and high-/low-frequency energy ratio in the EEG further verified proper separation to vigilance states (Fig. 2*D*). Taken together, prestimulus baseline activity confirmed that trials categorized as wakefulness, NREM sleep, and REM sleep, indeed, exhibited the behavioral and electrophysiological markers associated with these states, suggesting that normal sleep was largely preserved during auditory stimulation experiments.

Auditory Responses Are Largely Preserved Across Sleep States

As a first step for comparing activity triggered by sounds in wakefulness and sleep, evoked LFP responses were compared across vigilance states (Fig. 3). Average LFP responses in auditory cortex ($n = 160$ channels in 6 animals) had similar waveforms across vigilance states (Fig. 3*A*). However, despite the gross similarity, the amplitude of the initial component (negative peak 10–30 ms poststimulus) was highest in NREM sleep (-151 ± 12.5 μV), lower in wakefulness (-114 ± 9.6 μV), and lowest in REM sleep (-101 ± 8.4 μV), and these differences were statistically significant (ANOVA on amplitudes; $P < 0.0025$, $F > 6.2$ for vigilance state). In addition, NREM sleep was associated with a positive peak around 240 ms following stimulus onset (asterisk in Fig. 3*A*), corresponding to a poststimulus suppression of neuronal activity that was observed especially following high-intensity sounds. Average evoked MUA responses from the same auditory channels exhibited a clear onset response and a weaker offset response, and the intensity of both these responses was parametrically dependent on tone intensity (Fig. 3*B*). While sound intensity had a marked effect on MUA responses, there was no effect of vigilance state despite clear differences in baseline prestimulus levels (horizontal cyan line in Fig. 3*B*). A two-way analysis of variance (ANOVA) for MUA onset responses (10–30 ms) confirmed a highly significant main effect for sound intensity, $F_{1,102} = 412$, $P < 3.9\text{E}{-128}$, with no significant main effect of vigilance state, $F_{1,102} = 0.50$, $P > 0.6$ or interaction, $F_{1,102} = 0.49$, $P > 0.74$. In contrast to the robust responses observed in auditory cortex, LFP and MUA responses in frontal motor cortex were weak and inconsistent (Supplementary Fig. 3) thereby showing that responses in PAC were specific. However, the positive peak around 240 ms following stimulus onset during NREM sleep was observed also in motor cortex, suggesting that this late wave, reflecting poststimulus suppression, was a global phenomenon rather than being restricted to PAC alone. We also examined the muscle-tone changes evoked by auditory stimulation (Fig. 3*C*) to verify that auditory stimuli did not regularly wake up the animals. Auditory stimulation did not lead to long-lasting increases in muscle tone, as may be expected upon transition to wakefulness. Upon stimulation, high-intensity (80 dB SPL) tones were associated with average short-lasting (<100 ms) EMG changes. However, an analysis of single trials revealed that such phasic startle-like responses were only elicited in $3.6 \pm 1.0\%$ of trials (Materials and Methods). Importantly, no muscle-tone changes above baseline were observed for 30/55 dB SPL stimuli, and all the results reported here were also observed for these intensity levels.

Next, we examined auditory unit responses to all acoustic stimuli in the main experiment ($n = 295$; 152 single units and 143 mixed clusters). Unit responses were heterogeneous and included increases and (more rarely) decreases in firing around onset and offset of stimuli, as well as sustained responses throughout stimulus presentation, all of which were detected automatically (Fig. 4). Neuronal responses often showed selectivity to specific acoustic features of the auditory stimuli, for example, frequency tuning, preference for specific amplitude modulation rates, and tracking of temporal envelopes of the ultrasonic conspecific vocalizations (Supplementary Fig. 4); however, a detailed analysis of the precise acoustic features driving the responses is beyond the scope of this report. Analysis of onset response latencies (Fig. 5) revealed a unimodal distribution with short latencies (11.6 ± 0.3 ms). Of 295 auditory neurons, 194 (66%) exhibited a significant excitatory response to at least one stimulus ($q(\text{FDR}) < 0.05$ via *t*-test, Materials and Methods). Importantly, both the proportion of responsive neurons and their latencies are in line with recent studies of PAC in the rat (Polley et al. 2007) and therefore provide strong evidence that we recorded from PAC. Latencies of onset responses were not significantly different between vigilance states (one-way ANOVA on latency values; $P > 0.2$, $F = 1.6$). On average, during wakefulness units responded with onset, offset, and sustained increased responses to $21.2 \pm 1.7\%$, $7.6 \pm 1.3\%$, and $17.5 \pm 1.8\%$ of the suprathreshold stimuli, respectively (without considering the near-threshold 30-dB SPL stimuli).

Single-unit responses were then compared across vigilance states. Figure 6 shows representative auditory responses of a single unit (see Supplementary 5 for additional examples). As can be seen, neuronal responses were nearly indistinguishable visually across wakefulness and sleep states. We proceeded to compare quantitatively the selectivity as well as the magnitude of auditory responses across states (Materials and Methods). When comparing wakefulness with either NREM or REM sleep separately, both selectivity and response magnitude were largely comparable (Fig. 7). Specifically, the only case in which we detected significant differences in selectivity across vigilance states were onset responses, which were modestly (albeit significantly) greater in NREM sleep compared with wakefulness. Accordingly, there was a trend for neurons to respond to the onset of slightly more auditory stimuli in NREM sleep compared with wakefulness ($24.5 \pm 1.9\%$ vs. $21.2 \pm 1.7\%$ of stimuli). Given the large dataset, this difference was statistically significant ($P = 0.019$ via paired *t*-test), but was associated with a very weak effect size (Hedge's $g = -0.0123$) (Hentschke and Stuttgen 2011).

Similarly, all comparisons of response magnitude across states (quantified with spikes per second or alternatively expressed in percent of that state's baseline firing rate—not shown) could only reveal minor differences (e.g., maximal difference of 4.6% and 7.2% increased gain in wake versus NREM sleep and REM sleep, respectively, Fig. 7*C*). Given the large dataset, some of the pairwise comparisons of response magnitude reached statistical significance but were likewise associated with weak effect sizes (maximal Hedge's g value = 0.37). Along this line, when computing gain factors per unit instead of per stimulus, we found that the vast majority of neurons were not significantly modulated by vigilance state (71–88%, depending on the pair of vigilance states under comparison and the type of response, i.e., onset/offset/sustained), while a minority of units showed significant modulations in both directions. Given the similar results across vigilance states, we sought to verify that our analysis scheme was

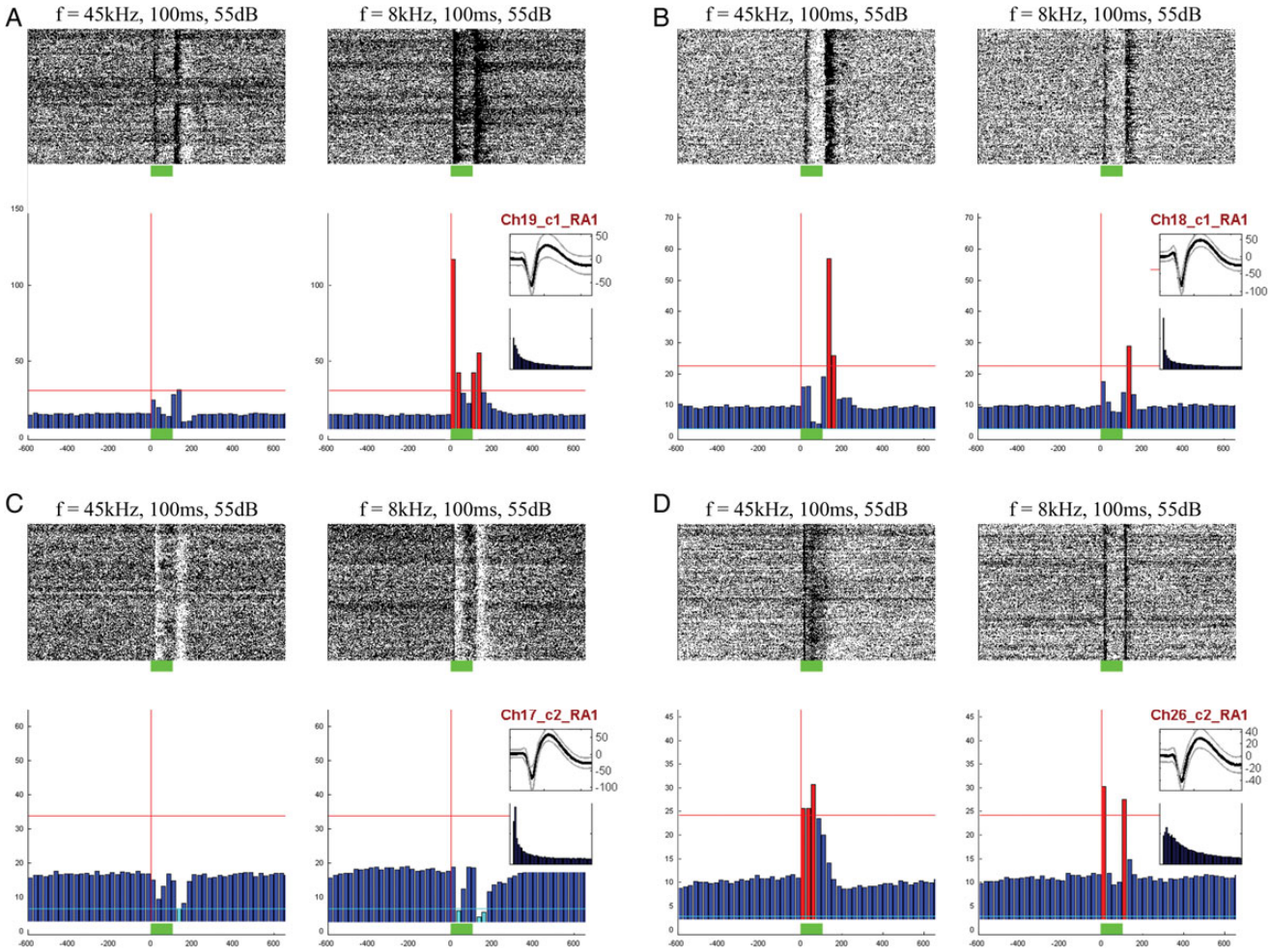

Figure 4. Types of auditory single-unit responses. Examples of different types of auditory responses to tones observed in 4 single units (*A–D*). In each panel, left and right columns show responses to tones with two different frequencies. Raster plots are shown above and PSTH below. Six types of responses were identified automatically (Materials and Methods) by considering increases and decreases in firing rates separately for onset, sustained, and offset responses. (*A*) This neuron responds to the 8-kHz tone (right) with a strong increased onset response and a weaker increased offset response. (*B*) This neuron mainly shows increased offset responses, more strongly to the 45-kHz tone. (*C*) This neuron shows decreased onset and offset responses to both tones (*D*) This neuron shows a sustained response to the 45-kHz tone and onset/offset responses to the 8-kHz tone. Red and cyan bars mark responses that were automatically detected and categorized as increases or decreases, respectively.

sufficiently sensitive to reveal differences when those were expected to be present. To this end, we compared response magnitudes in the first block of forced wakefulness (when neuronal firing rates were highest) with trials in NREM sleep. As expected, this control comparison revealed robust differences of 14–22% reduction in sleep (Supplementary Fig. 6), thereby demonstrating that the analysis employed was sufficiently sensitive. On the whole, single-unit auditory responses were largely preserved across sleep states. Differences in selectivity and magnitudes were on the order of few percent, associated with weak effect sizes, and rarely reached statistical significance.

Stimulus-specific Adaptation Is Largely Preserved Across Sleep States

To examine to what extent the processing of deviant tones may be different in sleep, we performed a second "oddball" experiment ($n = 8$ sessions) in which two 100-ms tones were presented either frequently (standard) or rarely (deviant) (Figs 8 and 9 and Materials and Methods). Average evoked responses to standard and deviant stimuli were first compared qualitatively across vigilance states (Fig. 8*B*). LFP-evoked responses ($n = 128$ channels in 5 animals) had higher amplitudes for deviant tones compared with standard tones. This difference, particularly expressed immediately following tone onset (10–30 ms), was largely comparable across wakefulness and sleep states (further quantification below). In contrast, late P3-like effects were absent or inconsistent in all vigilance states including wakefulness. MUA responses (Fig. 8*B*) and ERPs (recorded from screws attached the skull) similarly showed weaker responses following the onset of standard tones.

Next, we examined whether decreased responses to standard tones could be observed in the single-unit responses, and whether those effects were stimulus-specific. Figure 8*C* shows the responses of a representative PAC neuron during the oddball paradigm. As can be seen, this neuron responded strongly to low-frequency (8 kHz) tones, and to a lesser extent to high-frequency (45 kHz) tones. Onset responses were stronger for deviant stimuli, and this was especially the case for the preferred stimulus.

Next, SSA effects were quantified by computing a contrast between the "standard" responses and the "deviant" responses

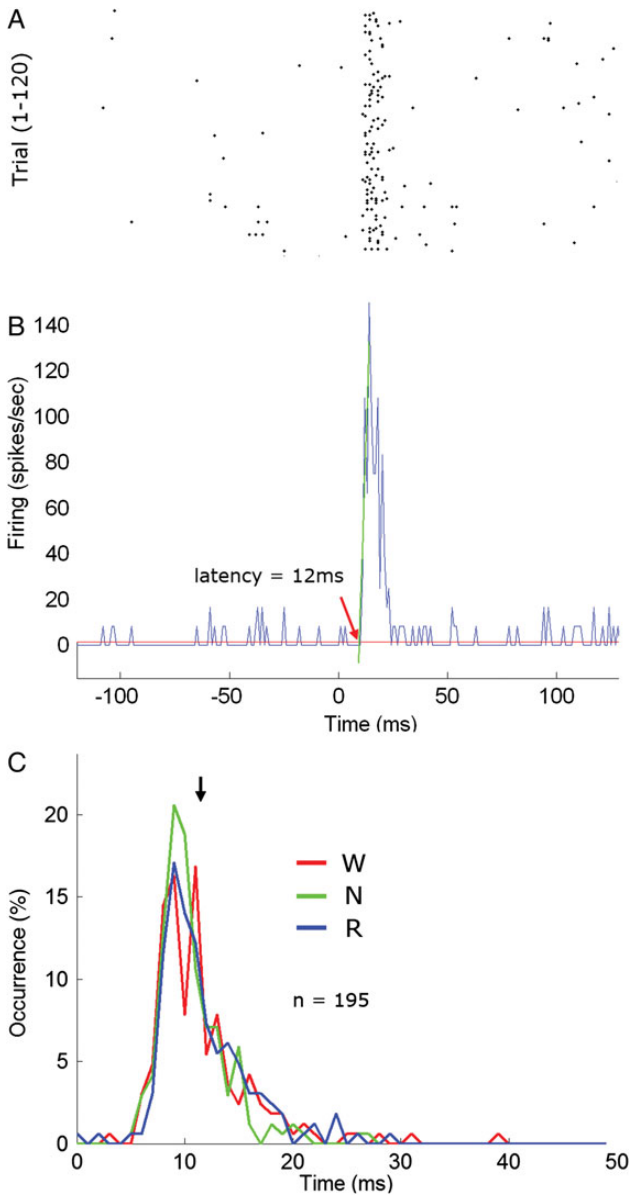

Figure 5. Latency of auditory single-unit onset responses. (*A*) Raster plot of an example single-unit excitatory onset response to 100-ms tone pips (8 kHz, 55 dB SPL). Each row is a trial (#1–120). (*B*) Corresponding peristimulus time histogram. The latency of onset responses was defined as in (Polley et al. 2007) as the intersection between the slope of the excitatory response profile (oblique green line) and the mean prestimulus baseline firing rate (horizontal red line). (*C*) Distribution of onset latencies across all auditory neurons exhibiting an excitatory onset response ($n = 195$). Red, green, and blue denote latencies during wakefulness, NREM sleep, and REM sleep, respectively. Black arrow denotes mean latency across all vigilance states (11.6 ms). Note that the distribution of response latencies is unimodal with 98% of latencies between 8 and 16 ms, in line with expected latencies in auditory core regions (Polley et al. 2007).

for the same tonal frequency, called the "SSA index" or SI (Materials and Methods). SIs were computed separately for LFP, MUA, and SUA ($n = 225$; 106 single-units and 119 mixed clusters) responses and separately for wakefulness, NREM sleep, and REM sleep (Fig. 9*A*). Across all vigilance states and in all signals used to quantify SSA (LFP, MUA, and SUA), both SI_1 and SI_2 tended to be mostly positive (gray shades in Fig. 9*A*), demonstrating that SSA was present throughout vigilance states. Finally, the common contrast between the deviant and standard responses was used to characterize the average effect of adaptation (CSI, see Materials and Methods). The distribution of common contrast CSI values in different vigilance states is shown in Figure 9*B* and was found to be entirely overlapping. Thus, our results show that the deviant tones elicit early SSA effects whose strength was similar across wakefulness and sleep states.

Discussion

In this study, we show that single-unit and LFP responses in core auditory cortex of unrestrained rats are comparable across wakefulness, NREM sleep, and REM sleep. Despite robust changes in baseline neuronal firing, baseline LFP power spectra and muscle tone across vigilance states, auditory responses across the neuronal population were largely preserved. Comparable results were revealed for response selectivity and response magnitude (when considered relative to that state's baseline firing rate or in terms of spikes per second), and this was true across different auditory stimuli (simple tones/clicks versus complex behaviorally relevant stimuli). All differences in selectivity and response magnitude between states were minimal (<8%) and the vast majority of comparisons did not reach statistical significance. We also examine for the first time the level of SSA following the onset of repetitive tones in natural sleep and demonstrate that the strength of such early (10–30 ms) effects in sleep (13–20% with our protocol) are comparable to those occurring during wakefulness. Taken together, the results demonstrate that despite the high arousal threshold brought about by sleep and the robust changes in electrical activity and neuromodulation between vigilance states, auditory responses in PAC are preserved—thereby supporting the notion that neuronal activity in primary sensory cortices is primarily driven by external physical stimuli with little modulation by vigilance state.

Comparison to Previous Studies

The present results differ from several previous studies in primates and cats that reported attenuated visual and somatosensory responses during NREM sleep (Evarts 1963; Gucer 1979; Livingstone and Hubel 1981). Similarly, early studies in the auditory cortex of cats and primates found neurons to be less responsive during NREM sleep (Murata and Kameda 1963; Brugge and Merzenich 1973). Rather, the current results extend the few recent single-unit studies in auditory cortex of guinea pigs and marmoset monkeys during natural sleep (Pena et al. 1999; Edeline et al. 2001; Issa and Wang 2008) that demonstrated comparable responses across vigilance states (Hennevin et al. 2007). One recent study (Issa and Wang 2011) demonstrated that NREM sleep reduced the sensitivity of auditory cortex to quiet sounds and reduced the extent of sound-evoked response suppression. In an attempt to consider these possibilities, we presented all sounds also at near-threshold levels of 30 dB SPL. However, the results did not reveal differences between vigilance states for such responses (see, e.g., black traces in Fig. 3*B* for MUA). Response suppressions were rare in our data and precluded systematic investigation of this aspect.

It is interesting to note the difference between evoked potentials and single-unit firing with respect to the comparison

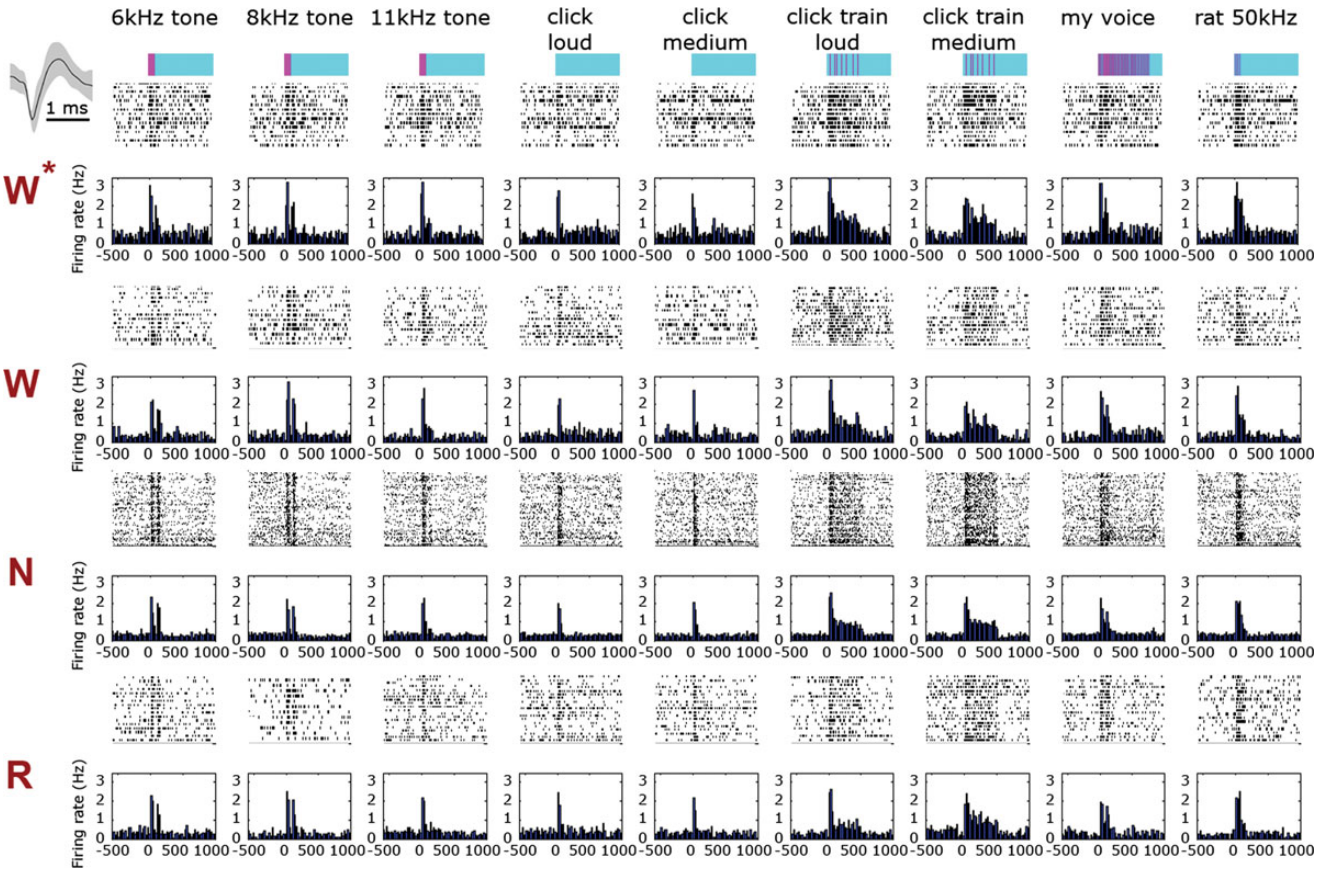

Figure 6. Representative auditory single-unit responses across vigilance states. (*A*) Representative auditory responses of a single-unit across vigilance states (rows) for 9 different stimuli (columns). Rows (top to bottom) correspond to stimuli names and intensities, timing and structure of acoustic stimulus (pink over cyan), followed by raster plots and PSTHs for each vigilance state. Inset on upper left shows mean ± SEM of action potential waveform. W*, first wake trials; W, wakefulness trials; N, NREM sleep trials; R, REM sleep trials. Firing rate in all bar graphs is expressed in terms of percent of wakefulness baseline and is shown with the same scale across all states and stimuli. Note that neuronal responses are nearly indistinguishable visually across vigilance states.

between vigilance states. The present results (Figs 3*A* and 8*B*) join previous studies in showing that NREM sleep is associated with larger amplitude-evoked potentials compared with wakefulness and REM sleep (Hall and Borbely 1970; Velluti 1997; Phillips et al. 2011), while single-unit responses do not exhibit such clear differences. Similarly, evoked potentials in human scalp EEG exhibit higher amplitudes during NREM sleep in response to auditory (Bastuji and Garcia-Larrea 1999; Colrain and Campbell 2007; Hennevin et al. 2007) or transcranial magnetic stimulation (Massimini et al. 2007). Given that the LFP is considered to reflect synaptic input (Mitzdorf 1985; Logothetis et al. 2001), a possible explanation is that during NREM sleep, synaptic input may not lead to differences in spiking activity. However, we believe that the discrepancy stems primarily from a difference in spatial scale—since the LFP captures combined neuronal activity in a volume of tissue (Nir et al. 2007, 2008). It is therefore possible that the response to the same stimulus recruits a larger neuronal population in NREM sleep, thereby giving rise to a larger amplitude potential in the LFP. Indeed, neurons were found here to be slightly, albeit significantly, less selective in NREM sleep, in accord also with human data showing decreased selectivity of auditory processing during NREM sleep (Perrin et al. 1999, 2002). Perhaps many neurons that contribute to an enhanced evoked response during NREM sleep are relatively inaccessible to extracellular recordings (e.g., smaller neurons in superficial layers with sparse firing). More generally, the LFP is more difficult to interpret than single-unit firing because of inherent summation of potentials from local and nonlocal sources and from different contributors (Buzsaki et al. 2012). Indeed, estimates of the size of the neuronal population giving rise to the LFP are highly disparate—ranging from several hundred micrometers [e.g., Katzner et al. (2009)] to a few millimeters [e.g., Logothetis et al. (2001)]. In addition, while postsynaptic currents are believed to be the most ubiquitous contributors to the LFP, many nonsynaptic currents may play important roles, including spike after hyperpolarizations and "down" states that are prevalent during NREM sleep (Buzsaki et al. 2012; Reimann et al. 2013). Future studies are needed to further explain the discrepancy between enhanced evoked responses in LFP/EEG and preserved single-unit spiking during NREM sleep.

The emerging notion from this and other recent single-unit studies is that both selectivity and magnitude of responses across the PAC population are comparable in both NREM and REM sleep to those observed during wakefulness, and this is the case for both simple stimuli (e.g., tones, clicks) as well as complex behaviorally relevant stimuli. In addition, variability exists between individual neurons in relation to the presence and direction of modulation between vigilance states, as reported here. The reasons underlying the discrepancy with

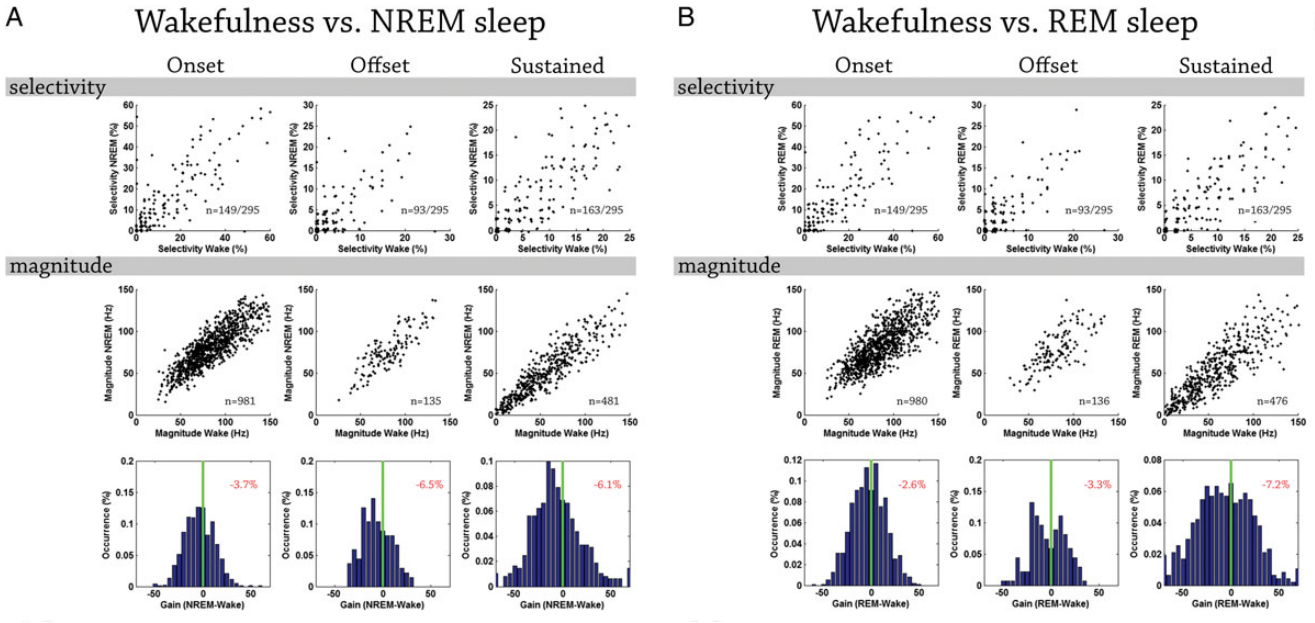

Figure 7. Quantitative comparison of auditory single-unit responses across vigilance states. (*A*) Quantitative comparison of auditory single-unit responses ($n = 295$) in wakefulness and NREM sleep. Columns (left to right) depict results for onset, offset, and sustained responses. Top row: scatter plot of selectivity (number of stimuli that trigger a response) in NREM sleep (*y*-axis) versus wakefulness (*x*-axis). Each dot denotes one auditory neuron ($n = 165$, 113, and 149 for onset, offset, and sustained responses in wakefulness, respectively). Middle row: scatter plot of response magnitudes (spikes per second) in NREM sleep (*y*-axis) versus wakefulness (*x*-axis). Each dot denotes the response of one neuron to a specific stimulus for which significant responses were identified in both vigilance states of interest ($n = 1345$, 209, and 356 conditions for onset, offset, and sustained responses, respectively). Red and green lines as above. Bottom row: distribution of gain factors computed for each stimulus separately. Vertical green line marks zero gain while percentage at top right corner shows the mean gain factor (none of these mean gain factors were significantly different than zero when evaluated via bootstrapping, see Supplementary Fig. 7). Positive (negative) gain values denote increased response magnitude in sleep (wakefulness). (*B*) Wakefulness versus REM sleep with format as in (*A*). Note that by and large single-unit responses in sleep retain comparable selectivity and response magnitudes.

earlier studies are not clear but one potential factor that could account for this variability is the laminar location of recordings. The present recordings were likely from granular and infragranular layers, although the precise laminar profile of each recording site is not available (see also Limitations).

Responses to Deviant Sounds in Oddball Paradigm

The processing of deviant tones was further compared in sleep and wakefulness using an oddball paradigm. The results reveal that the strength of SSA effects (13–20% with our protocol) were comparable across vigilance states thereby showing, for the first time, that early markers of deviance detection at the neuronal level persist during NREM and REM sleep states. Such comparable effects extend a growing body of literature suggesting that SSA in auditory cortex (and early deviance detection more generally) is not significantly modulated by behavioral state. Along this line, SSA in auditory cortex is readily observed in anesthetized cats (Ulanovsky et al. 2003), is observed in awake (von der Behrens et al. 2009; Farley et al. 2010) as well as anesthetized (Taaseh et al. 2011) rats, and evoked potentials recorded over cat auditory cortex reveal similar markers of deviance detection in wakefulness and NREM sleep (Csepe et al. 1987). SSA has been shown to be weak, rare, or nonexistent among neurons of the lemniscal pathway providing cortical input (Ulanovsky et al. 2003; Antunes et al. 2010), so that SSA in PAC (as measured here) is believed to be generated within cortex by local mechanisms (Ulanovsky et al. 2003) [but see also Antunes and Malmierca (2011)]. Depletion of synaptic vesicles in specific thalamocortical synapses may be an underlying mechanism, as SSA is expressed strongly already in thalamorecepient cortical layers (Szymanski et al. 2009).

Although early studies of SSA in the cat suggested that it could fully explain the generation of MMN, accumulating evidence suggests that this is not the case. Instead, single-unit SSA in PAC may lie upstream from neuronal processes generating the MMN and may contribute to earlier changes in the P1–N1 complex and/or other midlatency potentials (Nelken and Ulanovsky 2007; Winkler et al. 2009; Farley et al. 2010; Naatanen et al. 2011). This may help resolve the apparent discrepancy with the observation that in humans MMN is modulated as a function of vigilance state. Indeed, MMN is attenuated in sleep (Loewy et al. 1996; Ruby et al. 2008), under anesthesia (Heinke et al. 2004), and may undergo complex changes in patients with disorders of consciousness, although this is currently under debate (Bekinschtein et al. 2009; Boly et al. 2011; King et al. 2011).

No late effects such as MMN or P3-like potentials were observed in any state (including wakefulness) nor did we observe long-lasting changes in induced LFP power suggestive of reverberatory activity (not shown). The absence of late effects is in agreement with recent single-unit (von der Behrens et al. 2009) and ERP (Umbricht et al. 2005) studies in awake rodents but at odds with earlier studies describing differences occurring at 60–300 ms after stimulus onset (Yamaguchi et al. 1993; Shinba 1997; Ruusuvirta et al. 1998). Both stimulation parameters (e.g., probability of deviant tones and ISIs) and the passive oddball paradigm employed here may account for the absence of late P3-like effects, given that P3 amplitudes in

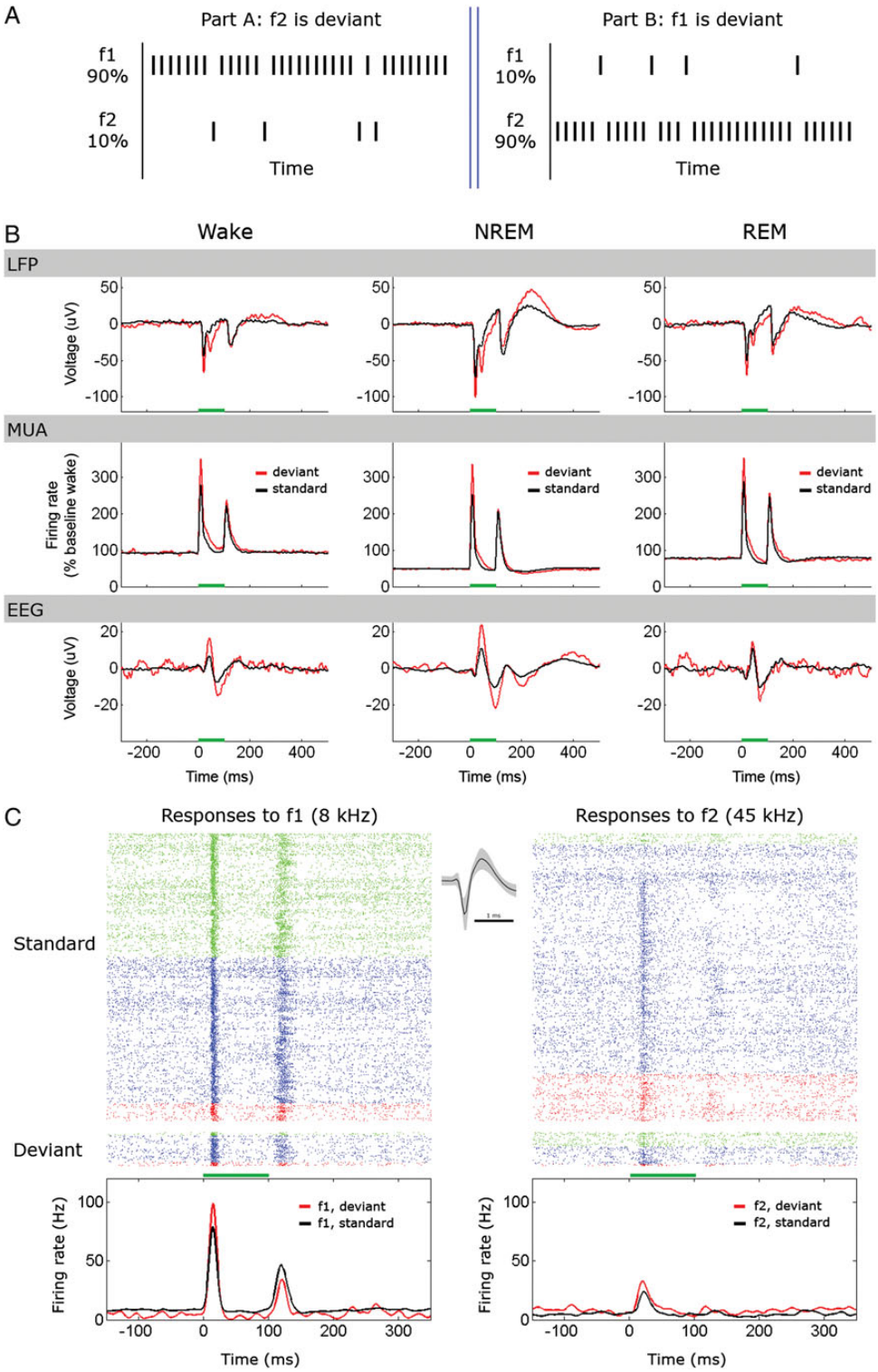

Figure 8. Oddball paradigm and stimulus-specific adaptation (SSA). (*A*) A schematic description of one block used in the oddball paradigm (each such block is repeated multiple times). A block consists of part A and part B. In each part, either f1 (8 kHz, 55 dB SPL) or f2 (45 kHz, 55 dB SPL) are presented pseudorandomly according to their probability of occurrence (90% for standard and 10% for deviant). (*B*) Average LFP responses (top), MUA responses (middle), and EEG responses (bottom) for standard (black) and deviant (red) stimuli across different vigilance states (columns); $n = 69\,300$ standard trials (16 632, 35 343, and 10 395 in Wake, NREM, and REM sleep, respectively) and 7700 deviant trials (2333, 4957, and 1458 in Wake, NREM, and REM sleep, respectively), 8 recording sessions in 5 animals. Note that an enhanced early response to deviant tones persists across sleep states. (*C*) Representative responses of one single unit during the oddball paradigm across all vigilance states. The raster plot shows 4050 presentations for the standard tone (top) and 450 presentations for the oddball tone (bottom), separately for f1 (left) and f2 (right). Red, green, and blue ticks denote action potentials during wakefulness, NREM sleep, and REM sleep, respectively. Line graphs (bottom) show PSTHs smoothed by a 5-ms Hamming window. Note that this neuron responds preferentially to f1 but exhibits enhanced early responses to both stimuli. Horizontal green bars mark stimulus.

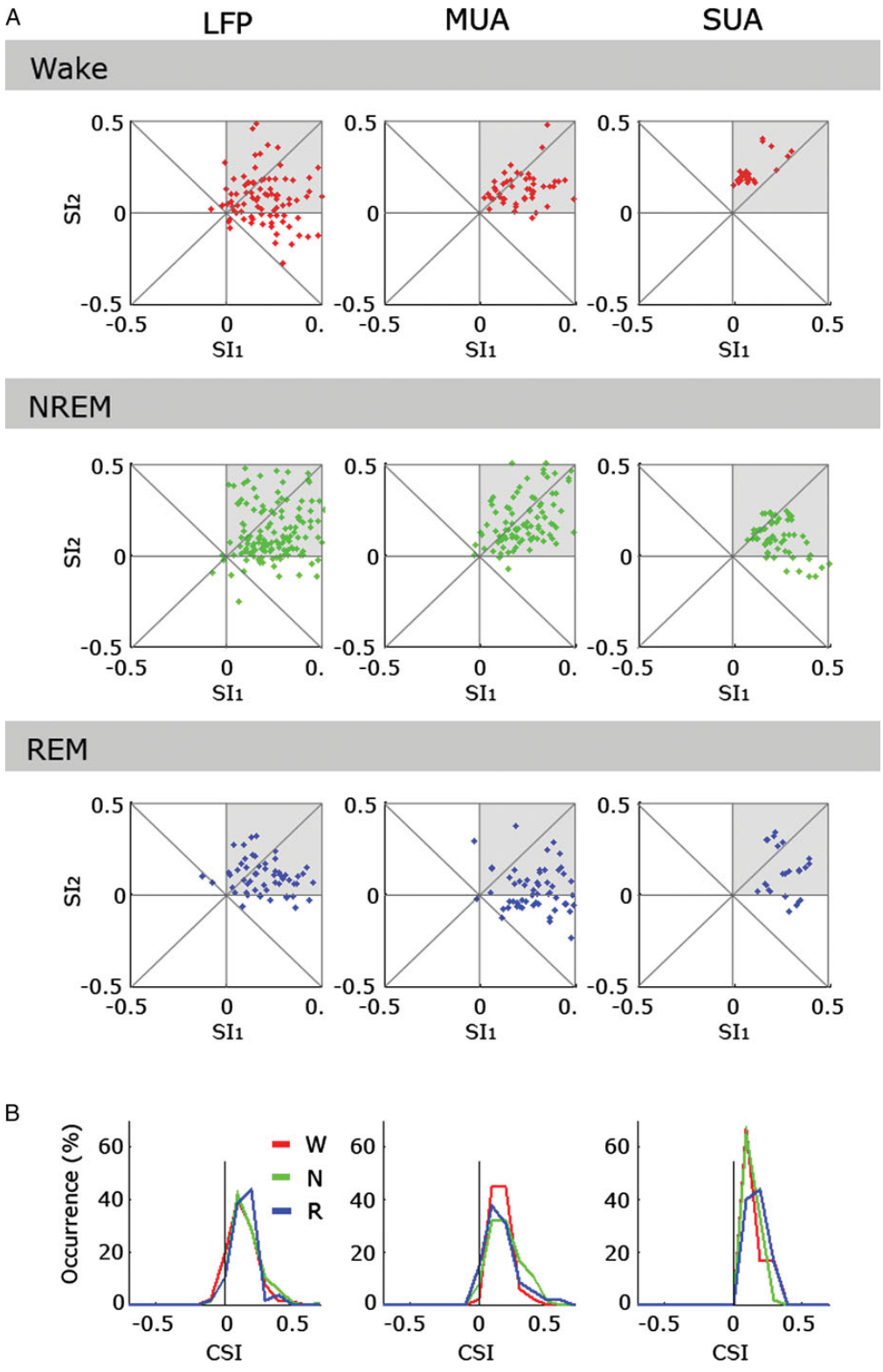

Figure 9. Quantitative comparison of SSA across vigilance states. (*A*) Scatter plots of SI_2 (SSA index for f2 = 45 kHz, 55 dB SPL), versus SI_1 (SSA index for f1 = 8 kHz, 55 dB SPL) for neuronal responses measured in LFP, MUA, and SUA (columns, left to right) separately during wakefulness, NREM sleep and REM sleep (rows, top to bottom). Note that most responses show some SSA for both f1 and f2 (upper right quadrant in each scatter plot, gray shade. (*B*) Histograms of common SSA index (CSI across both frequencies, Materials and Methods) for LFP, MUA, and SUA (columns, left to right). Red, green, and blue traces mark the superimposed distributions for wakefulness, NREM sleep, and REM sleep, respectively. Note that SSA indices are comparable across vigilance states.

the rat are markedly enhanced in active conditions when rare tones are associated with rewards or aversive outcomes through training (Shinba 1997; Sambeth et al. 2003).

On the whole, given that comparable SSA effects were found here across wakefulness and sleep in the absence of late MMN or P3-like potentials, the results support the notion that

SSA is a marker of neuronal activity occurring earlier than global integrative processes generating the MMN. Thus, comparable SSA across wakefulness and sleep is best interpreted as evidence that processes occurring within 50 ms of stimulus onset within core auditory cortex are primarily driven by physical stimuli with little modulation by vigilance state.

Relation to Functional Imaging Studies in Humans

In humans, evoked potential studies have shown robust activation in response to sounds during sleep (Nielsen-Bohlman et al. 1991; Bastuji et al. 2002; Cote 2002; Colrain and Campbell 2007; Hennevin et al. 2007). Similarly, most other fMRI studies of auditory stimulation during NREM sleep (Portas et al. 2000; Dang-Vu et al. 2011) have found that in auditory regions along temporal cortex, responses resemble those found during wakefulness. On the other hand, a few studies report reduced activity in auditory cortex during sleep (Czisch et al. 2002, 2004), and others have noted that stimulation at times when sleep spindles occur may result in different responses (Dang-Vu et al. 2011; Schabus et al. 2012). By and large, the present single-unit results confirm the former set of findings at the neuronal level, but conflicting results and their relation to single-unit measures are difficult to resolve since BOLD fMRI measurements reflect average activity over large neuronal populations and over time intervals of seconds. Indeed, fMRI in human auditory cortex primarily reflects distributed correlated activity (Nir et al. 2007) while the present results and other single-unit data show that, at a fine neural scale, sleep affects auditory cortical responses in a heterogeneous manner (Pena et al. 1999; Edeline et al. 2001; Issa and Wang 2008). Temporally, auditory stimulation and particularly high-intensity (loud) sounds used in many imaging studies (given MR scanner noise) can often lead to an induced poststimulus "OFF" period as we observe here (Fig. 3*B*). In such cases, BOLD signals in sleep may often reflect integration over a (preserved) response and a poststimulus suppression.

Overall, human studies suggest that the main differences between wakefulness and sleep are found at later processing stages, in terms of both timing and cortical hierarchy, and may depend on altered intercortical connectivity. With fMRI, it was found that despite comparable responses in PAC, auditory stimuli are not as effective in driving the activity of high-order (e.g., parietal and prefrontal) regions (Portas et al. 2000). Also, despite the existence of human ERPs to oddball stimuli in sleep (Niiyama et al. 1994, 1999, 2000; Ruby et al. 2008), the magnitude and spatial extent of late P3 may be reduced during sleep (Cote 2002; Colrain and Campbell 2007). Along this line, a functional cortical disconnection during sleep (Massimini et al. 2005) may prevent activity in primary sensory regions from effectively driving higher order cortical regions. Modeling studies suggest that NREM sleep may be associated with diminished intercortical transmission (Esser et al. 2009), possibly mediated by local OFF periods (Nir et al. 2011) that could block signal propagation. In REM sleep, there also seems to be dissociation of primary visual cortex (V1) from high-order visual regions (Braun et al. 1998). Overall, the possibility that primary sensory regions cannot effectively drive high-order activity in sleep highlights the importance of recording sensory responses simultaneously from multiple cortical areas in future studies.

Sleep and Anesthesia

Both sleep and anesthesia entail behavioral and perceptual disconnection from external sensory stimuli. In addition, under anesthesia and in NREM sleep, hyperpolarized neurons in the thalamocortical system become bistable and give rise to slow oscillations (Steriade et al. 1993, 2001). For these reasons and for practical considerations (such as better control and easier data collection), results from anesthetized preparations are often used as an analogy to sleep (Timofeev et al. 1996). Anesthesia has been shown to reduce responses in auditory cortex, especially for sustained responses (Brugge and Merzenich 1973; DeWeese et al. 2003) and this raises the possibility that similar processes (along with possible thalamic gating) underlie sleep disconnection. How could the comparable PAC responses reported here (observed also for sustained responses) be explained in light of these findings? Using the state of anesthesia as a model for natural sleep is an oversimplification [see Hennevin et al. (2007) for review]. First, anesthesia is heterogeneous and may lead to disconnection and unconsciousness via distinct pathways. While certain "dissociative" anesthetics such as ketamine lead to unresponsiveness with some preserved conscious dream-like experience, other anesthetics including volatile agents, urethane, and barbiturates globally deactivate brain activity in a manner that is more akin to NREM sleep (Alkire et al. 2008). Second, studies directly comparing responses in natural sleep with GABA-agonist anesthetics in rodents and cats have noted important difference in responses (Cotillon-Williams and Edeline 2003), and it is especially clear that responses during REM sleep exhibit marked differences in comparison to anesthesia (Kishikawa et al. 1995; Torterolo et al. 2002). Indeed, in REM sleep, the thalamocortical system is depolarized, neurons fire tonically, and low-amplitude high-frequency activity prevails in the LFPs and in the EEG. Despite this strong cortical activation, a high arousal threshold persists in REM sleep. Thus, disconnection during sleep, and REM sleep in particular, cannot be explained by considering anesthesia. Given the strong cortical activation, REM sleep disconnection poses a highly intriguing unsolved paradox.

Limitations

Identification of Cortical Auditory Fields

Core (primary) auditory cortex was identified based on histology, neural responsiveness, and short unimodal latency distribution but the definition did not include a full tonotopic mapping or a comparison of responses to pure tones versus noise stimuli. However, this limitation should not affect the conclusions since 1) the vast majority of responses are in PAC, so conclusions about PAC should not be affected by additional recordings outside PAC; 2) if cortical recording sites that were potentially outside PAC nevertheless show comparable responses across wakefulness and sleep, it may strengthen the notion that in PAC responses are largely preserved.

Free-field Stimulation

Sounds were played in a free-field configuration as unrestrained animals were behaving freely in their home cages. Consequently, slight differences in location and posture may affect the exact levels of sounds in each trial. This may have potentially confounded a result of a significant difference between vigilance states (e.g., if during sleep a typical posture leads to weaker stimulation) but given the observed comparable responses this limitation should not affect the conclusions.

Electrophysiological Recordings

Our extracellular recordings were not ideal for reliable discrimination between the discharges of excitatory and inhibitory neurons, nor could the precise laminar location be determined in each recording site. Based on 1) those cases where histology permitted identification of laminar locations, 2) baseline firing rates, 3) the proportion of responsive neurons, and 4) the polarity of locally recorded sleep slow waves in comparison to those recorded on the skull, it is likely that most recordings tended to be in middle/infragranular layers (Sakata and Harris 2009). Future studies employing laminar recordings during natural sleep could determine whether specific neuronal populations may modulate their activity patterns as a function of vigilance states. With regards to stability of recordings, the sleep in rodents provides an advantage over studies in primates and humans, since vigilance states were interleaved throughout the recording session rather than one state typically occurring before another (e.g., wakefulness before NREM sleep) thereby confounding a comparison of states with stability issues.

Potential Inattention During Wakefulness

It could be that the comparable auditory responses observed here can be explained in part by a state of inattentiveness during wakefulness, since sounds were not associated with behavioral outcomes (reward/aversive outcome) through training. In animal studies, the effects of attention in auditory cortex seem weak or variable (Miller et al. 1972; Benson and Hienz 1978) but attention can robustly modulate activity in human auditory cortex, especially when directed toward other sensory events such as visual stimuli (Fritz et al. 2007; Zatorre 2007). Ultimately, this issue can be best clarified by conducting human studies in which cognitive variables are carefully manipulated and compared with the effects of vigilance states in the same participants.

Functional Significance and Future Directions

The present results join other studies (Pena et al. 1999; Edeline et al. 2001; Issa and Wang 2008) in suggesting that ascending signals along the auditory pathway drive overall activity in PAC during sleep much as they typically do during wakefulness. One possibility is that this may not be the case in other modalities (i.e., somatosensory, visual) where responses in primary cortical regions may be attenuated (Evarts 1963; Gucer 1979; Livingstone and Hubel 1981). If so, audition may serve a unique adaptive protective role by monitoring distant events in the environment during an otherwise disconnected state of sleep. Alternatively, comparable activity in primary sensory regions across all modalities is not sufficient for external sensory to be regularly perceived and elicit behavioral responses during sleep. Cortical functional disconnection, possibly triggered by a distinct neuromodulatory milieu in sleep, may prevent activity in primary sensory regions to effectively drive high-level regions and future studies are required to investigate signal propagation simultaneously across cortical regions and layers. It remains to be seen whether similar mechanisms underlie disconnection in NREM and REM sleep despite their different electrical and neuromodulatory activities. One aspect that holds true for both NREM and REM sleep is reduced activity of the locus coeruleus–norepinephrine (LC–NE) system (Jones 2005), and this may play a key role in maintaining disconnection. Indeed, during wakefulness LC–NE activity is implicated in orienting toward behaviorally relevant sensory stimuli and is related to evoked potentials such as the P3 (Nieuwenhuis et al. 2005) which are well correlated with perceptual awareness (Dehaene and Changeux 2011).

Overall, the present results provide a "lower bound" on the search for mechanisms that underlie sleep disconnection, in terms of candidate brain regions and time intervals in which processing differences may occur. Understanding if, where, when and in what ways processing of sensory stimuli differs in sleep will help explain the disconnection that is a defining feature of sleep. More generally, it can help elucidate the effects of state-dependent cortical processing, the relation between consciousness and underlying brain activity, and the neural basis of neurological and psychiatric disorders that involve disconnection including attention disorders, dementia, schizophrenia, autism, and disorders of consciousness.

Supplementary Material

Supplementary can be found at: http://www.cercor.oxfordjournals.org/.

Funding

This work was supported by the National Institute of Health Director's Pioneer Award to G.T., the Human Frontier Science Program Organization long-term fellowship to Y.N., and the I-CORE Program of the Planning and Budgeting Committee and The Israel Science Foundation (grant No. 51/11) to Y.N.

Notes

We thank John Brugge, Israel Nelken, and Giovanni Santostasi for help with acoustic setup and calibration. Paul Pool for AM and FM sounds. Justin Williams, Tom Richner, and Sarah Brodnick for electrodes and surgical procedures. Peter Magill for DiI protocols. Marie-Eve Tremblay, Luisa De-Vivo, and Martha Pfister-Genskow for help with histology. Melissa Luck for soundproof chamber. Chadd Funk for comments on earlier drafts. *Conflict of Interest:* None declared.

References

Alkire MT, Hudetz AG, Tononi G. 2008. Consciousness and anesthesia. Science. 322:876–880.

Antunes FM, Malmierca MS. 2011. Effect of auditory cortex deactivation on stimulus-specific adaptation in the medial geniculate body. J Neurosci. 31:17306–17316.

Antunes FM, Nelken I, Covey E, Malmierca MS. 2010. Stimulus-specific adaptation in the auditory thalamus of the anesthetized rat. PLoS One. 5:e14071.

Artieda J, Valencia M, Alegre M, Olaziregi O, Urrestarazu E, Iriarte J. 2004. Potentials evoked by chirp-modulated tones: a new technique to evaluate oscillatory activity in the auditory pathway. Clin Neurophysiol. 115:699–709.

Bastuji H, Garcia-Larrea L. 1999. Evoked potentials as a tool for the investigation of human sleep. Sleep Med Rev. 3:23–45.

Bastuji H, Perrin F, Garcia-Larrea L. 2002. Semantic analysis of auditory input during sleep: studies with event related potentials. Int J Psychophysiol. 46:243–255.

Bekinschtein TA, Dehaene S, Rohaut B, Tadel F, Cohen L, Naccache L. 2009. Neural signature of the conscious processing of auditory regularities. Proc Natl Acad Sci USA. 106:1672–1677.

Benjamini Y, Yekutieli D. 2001. The control of the false discovery rate in multiple testing under dependency. Ann Stat. 29:1165–1188.

Benson DA, Hienz RD. 1978. Single-unit activity in the auditory cortex of monkeys selectively attending left vs. right ear stimuli. Brain Res. 159:307–320.
Boly M, Garrido MI, Gosseries O, Bruno MA, Boveroux P, Schnakers C, Massimini M, Litvak V, Laureys S, Friston K. 2011. Preserved feedforward but impaired top-down processes in the vegetative state. Science. 332:858–862.
Braun AR, Balkin TJ, Wesensten NJ, Gwadry F, Carson RE, Varga M, Baldwin P, Belenky G, Herscovitch P. 1998. Dissociated pattern of activity in visual cortices and their projections during human rapid eye movement sleep. Science. 279:91–95.
Brugge JF, Merzenich MM. 1973. Responses of neurons in auditory cortex of the macaque monkey to monaural and binaural stimulation. J Neurophysiol. 36:1138–1158.
Buzsaki G, Anastassiou CA, Koch C. 2012. The origin of extracellular fields and currents—EEG, ECoG, LFP and spikes. Nat Rev Neurosci. 13:407–420.
Colrain IM, Campbell KB. 2007. The use of evoked potentials in sleep research. Sleep Med Rev. 11:277–293.
Costa-Faidella J, Grimm S, Slabu L, Diaz-Santaella F, Escera C. 2011. Multiple time scales of adaptation in the auditory system as revealed by human evoked potentials. Psychophysiology. 48:774–783.
Cote KA. 2002. Probing awareness during sleep with the auditory odd-ball paradigm. Int J Psychophysiol. 46:227–241.
Cotillon-Williams N, Edeline JM. 2003. Evoked oscillations in the thalamo-cortical auditory system are present in anesthetized but not in unanesthetized rats. J Neurophysiol. 89:1968–1984.
Csepe V, Karmos G, Molnar M. 1987. Evoked potential correlates of stimulus deviance during wakefulness and sleep in cat—animal model of mismatch negativity. Electroencephalogr Clin Neurophysiol. 66:571–578.
Czisch M, Wehrle R, Kaufmann C, Wetter TC, Holsboer F, Pollmacher T, Auer DP. 2004. Functional MRI during sleep: BOLD signal decreases and their electrophysiological correlates. Eur J Neurosci. 20:566–574.
Czisch M, Wetter TC, Kaufmann C, Pollmacher T, Holsboer F, Auer DP. 2002. Altered processing of acoustic stimuli during sleep: reduced auditory activation and visual deactivation detected by a combined fMRI/EEG study. Neuroimage. 16:251–258.
Dang-Vu TT, Bonjean M, Schabus M, Boly M, Darsaud A, Desseilles M, Degueldre C, Balteau E, Phillips C, Luxen A et al. 2011. Interplay between spontaneous and induced brain activity during human non-rapid eye movement sleep. Proc Natl Acad Sci USA. 108: 15438–15443.
Dehaene S, Changeux JP. 2011. Experimental and theoretical approaches to conscious processing. Neuron. 70:200–227.
DeWeese MR, Wehr M, Zador AM. 2003. Binary spiking in auditory cortex. J Neurosci. 23:7940–7949.
Doron NN, Ledoux JE, Semple MN. 2002. Redefining the tonotopic core of rat auditory cortex: physiological evidence for a posterior field. J Comp Neurol. 453:345–360.
Edeline JM, Dutrieux G, Manunta Y, Hennevin E. 2001. Diversity of receptive field changes in auditory cortex during natural sleep. Eur J Neurosci. 14:1865–1880.
Esser SK, Hill SL, Tononi G. 2009. Breakdown of effective connectivity during slow wave sleep: investigating the mechanism underlying a cortical gate using large-scale modeling. J Neurophysiol. 102:2096–2111.
Evarts EV. 1963. Photically evoked responses in visual cortex units during sleep and waking. J Neurophysiol. 26:229–248.
Farley BJ, Quirk MC, Doherty JJ, Christian EP. 2010. Stimulus-specific adaptation in auditory cortex is an NMDA-independent process distinct from the sensory novelty encoded by the mismatch negativity. J Neurosci. 30:16475–16484.
Fritz JB, Elhilali M, David SV, Shamma SA. 2007. Auditory attention—focusing the searchlight on sound. Curr Opin Neurobiol. 17: 437–455.
Gucer G. 1979. The effect of sleep upon the transmission of afferent activity in the somatic afferent system. Exp Brain Res. 34:287–298.
Hall RD, Borbely AA. 1970. Acoustically evoked potentials in the rat during sleep and waking. Exp Brain Res. 11:93–110.
Heinke W, Kenntner R, Gunter TC, Sammler D, Olthoff D, Koelsch S. 2004. Sequential effects of increasing propofol sedation on frontal and temporal cortices as indexed by auditory event-related potentials. Anesthesiology. 100:617–625.
Hennevin E, Huetz C, Edeline JM. 2007. Neural representations during sleep: from sensory processing to memory traces. Neurobiol Learn Mem. 87:416–440.
Hentschke H, Stuttgen MC. 2011. Computation of measures of effect size for neuroscience data sets. Eur J Neurosci. 34:1887–1894.
Issa EB, Wang X. 2008. Sensory responses during sleep in primate primary and secondary auditory cortex. J Neurosci. 28: 14467–14480.
Issa EB, Wang X. 2011. Altered neural responses to sounds in primate primary auditory cortex during slow-wave sleep. J Neurosci. 31:2965–2973.
Jones BE. 2005. From waking to sleeping: neuronal and chemical substrates. Trends Pharmacol Sci. 26:578–586.
Katzner S, Nauhaus I, Benucci A, Bonin V, Ringach DL, Carandini M. 2009. Local origin of field potentials in visual cortex. Neuron. 61:35–41.
Keller GB, Bonhoeffer T, Hubener M. 2012. Sensorimotor mismatch signals in primary visual cortex of the behaving mouse. Neuron. 74:809–815.
King JR, Bekinschtein T, Dehaene S. 2011. Comment on "Preserved feedforward but impaired top-down processes in the vegetative state". Science. 334:1203; author reply 1203.
Kishikawa K, Uchida H, Yamamori Y, Collins JG. 1995. Low-threshold neuronal activity of spinal dorsal horn neurons increases during REM sleep in cats: comparison with effects of anesthesia. J Neurophysiol. 74:763–769.
Kralik JD, Dimitrov DF, Krupa DJ, Katz DB, Cohen D, Nicolelis MA. 2001. Techniques for long-term multisite neuronal ensemble recordings in behaving animals. Methods. 25:121–150.
Livingstone MS, Hubel DH. 1981. Effects of sleep and arousal on the processing of visual information in the cat. Nature. 291:554–561.
Loewy DH, Campbell KB, Bastien C. 1996. The mismatch negativity to frequency deviant stimuli during natural sleep. Electroencephalogr Clin Neurophysiol. 98:493–501.
Logothetis NK, Pauls J, Augath M, Trinath T, Oeltermann A. 2001. Neurophysiological investigation of the basis of the fMRI signal. Nature. 412:150–157.
Magill PJ, Pogosyan A, Sharott A, Csicsvari J, Bolam JP, Brown P. 2006. Changes in functional connectivity within the rat striatopallidal axis during global brain activation in vivo. J Neurosci. 26:6318–6329.
Mariotti M, Formenti A, Mancia M. 1989. Responses of VPL thalamic neurones to peripheral stimulation in wakefulness and sleep. Neurosci Lett. 102:70–75.
Massimini M, Ferrarelli F, Esser SK, Riedner BA, Huber R, Murphy M, Peterson MJ, Tononi G. 2007. Triggering sleep slow waves by transcranial magnetic stimulation. Proc Natl Acad Sci USA. 104: 8496–8501.
Massimini M, Ferrarelli F, Huber R, Esser SK, Singh H, Tononi G. 2005. Breakdown of cortical effective connectivity during sleep. Science. 309:2228–2232.
McCormick DA, Bal T. 1994. Sensory gating mechanisms of the thalamus. Curr Opin Neurobiol. 4:550–556.
McDonald DG, Schicht WW, Frazier RE, Shallenberger HD, Edwards DJ. 1975. Studies of information processing in sleep. Psychophysiology. 12:624–629.
Miller JM, Sutton D, Pfingst B, Ryan A, Beaton R, Gourevitch G. 1972. Single cell activity in the auditory cortex of Rhesus monkeys: behavioral dependency. Science. 177:449–451.
Mitzdorf U. 1985. Current source-density method and application in cat cerebral cortex: investigation of evoked potentials and EEG phenomena. Physiol Rev. 65:37–100.
Mukhametov LM, Rizzolatti G. 1970. The responses of lateral geniculate neurons to flashes of light during the sleep-waking cycle. Arch Ital Biol. 108:348–368.
Murata K, Kameda K. 1963. The activity of single cortical neurones of unrestrained cats during sleep and wakefulness. Arch Ital Biol. 101:306–331.

Naatanen R, Kujala T, Winkler I. 2011. Auditory processing that leads to conscious perception: a unique window to central auditory processing opened by the mismatch negativity and related responses. Psychophysiology. 48:4–22.
Neckelmann D, Ursin R. 1993. Sleep stages and EEG power spectrum in relation to acoustical stimulus arousal threshold in the rat. Sleep. 16:467–477.
Nelken I, Ulanovsky N. 2007. Mismatch negativity and stimulus-specific adaptation in animal models. J Psychophysiol. 21:214–223.
Nielsen-Bohlman L, Knight RT, Woods DL, Woodward K. 1991. Differential auditory processing continues during sleep. Electroencephalogr Clin Neurophysiol. 79:281–290.
Nieuwenhuis S, Aston-Jones G, Cohen JD. 2005. Decision making, the P3, and the locus coeruleus-norepinephrine system. Psychol Bull. 131:510–532.
Niiyama Y, Fujiwara R, Satoh N, Hishikawa Y. 1994. Endogenous components of event-related potential appearing during NREM stage 1 and REM sleep in man. Int J Psychophysiol. 17:165–174.
Nir Y, Dinstein I, Malach R, Heeger DJ. 2008. BOLD and spiking activity. Nat Neurosci. 11:523–524.
Nir Y, Fisch L, Mukamel R, Gelbard-Sagiv H, Arieli A, Fried I, Malach R. 2007. Coupling between neuronal firing rate, gamma LFP, and BOLD fMRI is related to interneuronal correlations. Curr Biol. 17:1275–1285.
Nir Y, Tononi G. 2010. Dreaming and the brain: from phenomenology to neurophysiology. Trends Cogn Sci. 14:88–100.
Nir Y, Staba RJ, Andrillon T, Vyazovskiy VV, Cirelli C, Fried I, Tononi G. 2011. Regional slow waves and spindles in human sleep. Neuron. 70:153–169.
Oswald I, Taylor AM, Treisman M. 1960. Discriminative responses to stimulation during human sleep. Brain. 83:440–453.
Paxinos G, Watson C. 1986. The rat brain in stereotaxic coordinates. 2nd ed. Amsterdam: Elsevier.
Pena JL, Perez-Perera L, Bouvier M, Velluti RA. 1999. Sleep and wakefulness modulation of the neuronal firing in the auditory cortex of the guinea pig. Brain Res. 816:463–470.
Perrin F, Bastuji H, Garcia-Larrea L. 2002. Detection of verbal discordances during sleep. Neuroreport. 13:1345–1349.
Perrin F, Bastuji H, Mauguiere F, Garcia-Larrea L. 2000. Functional dissociation of the early and late portions of human K-complexes. Neuroreport. 11:1637–1640.
Perrin F, Garcia-Larrea L, Mauguiere F, Bastuji H. 1999. A differential brain response to the subject's own name persists during sleep. Clin Neurophysiol. 110:2153–2164.
Phillips DJ, Schei JL, Meighan PC, Rector DM. 2011. State-dependent changes in cortical gain control as measured by auditory evoked responses to varying intensity stimuli. Sleep. 34:1527–1537.
Polley DB, Read HL, Storace DA, Merzenich MM. 2007. Multiparametric auditory receptive field organization across five cortical fields in the albino rat. J Neurophysiol. 97:3621–3638.
Portas CM, Krakow K, Allen P, Josephs O, Armony JL, Frith CD. 2000. Auditory processing across the sleep-wake cycle: simultaneous EEG and fMRI monitoring in humans. Neuron. 28:991–999.
Quian Quiroga R, Nadasdy Z, Ben-Shaul Y. 2004. Unsupervised spike sorting with wavelets and superparamagnetic clustering. Neural Comput. 16:1661–1687.
Rechtschaffen A. 1978. The single-mindedness and isolation of dreams. Sleep. 1:97–109.
Rechtschaffen A, Hauri P, Zeitlin M. 1966. Auditory awakening thresholds in REM and NREM sleep stages. Percept Mot Skills. 22:927–942.
Reimann MW, Anastassiou CA, Perin R, Hill SL, Markram H, Koch C. 2013. A biophysically detailed model of neocortical local field potentials predicts the critical role of active membrane currents. Neuron. 79:375–390.
Ruby P, Caclin A, Boulet S, Delpuech C, Morlet D. 2008. Odd sound processing in the sleeping brain. J Cogn Neurosci. 20:296–311.
Ruusuvirta T, Penttonen M, Korhonen T. 1998. Auditory cortical event-related potentials to pitch deviances in rats. Neurosci Lett. 248:45–48.
Sakata S, Harris KD. 2009. Laminar structure of spontaneous and sensory-evoked population activity in auditory cortex. Neuron. 64:404–418.
Sambeth A, Maes JH, Van Luijtelaar G, Molenkamp IB, Jongsma ML, Van Rijn CM. 2003. Auditory event-related potentials in humans and rats: effects of task manipulation. Psychophysiology. 40:60–68.
Schabus M, Dang-Vu TT, Heib DP, Boly M, Desseilles M, Vandewalle G, Schmidt C, Albouy G, Darsaud A, Gais S et al. 2012. The fate of incoming stimuli during NREM sleep is determined by spindles and the phase of the slow oscillation. Front Neurol. 3:40.
Shinba T. 1997. Event-related potentials of the rat during active and passive auditory oddball paradigms. Electroencephalogr Clin Neurophysiol. 104:447–452.
Steriade M. 2003. Neuronal substrates of sleep and epilepsy. Cambridge, UK: Cambridge University Press.
Steriade M, Nunez A, Amzica F. 1993. A novel slow (<1 Hz) oscillation of neocortical neurons in vivo: depolarizing and hyperpolarizing components. J Neurosci. 13:3252–3265.
Steriade M, Timofeev I, Grenier F. 2001. Natural waking and sleep states: a view from inside neocortical neurons. J Neurophysiol. 85:1969–1985.
Szymanski FD, Garcia-Lazaro JA, Schnupp JW. 2009. Current source density profiles of stimulus-specific adaptation in rat auditory cortex. J Neurophysiol. 102:1483–1490.
Taaseh N, Yaron A, Nelken I. 2011. Stimulus-specific adaptation and deviance detection in the rat auditory cortex. PLoS One. 6: e23369.
Timofeev I, Contreras D, Steriade M. 1996. Synaptic responsiveness of cortical and thalamic neurones during various phases of slow sleep oscillation in cat. J Physiol. 494(Pt 1):265–278.
Torterolo P, Falconi A, Morales-Cobas G, Velluti RA. 2002. Inferior colliculus unitary activity in wakefulness, sleep and under barbiturates. Brain Res. 935:9–15.
Ulanovsky N, Las L, Nelken I. 2003. Processing of low-probability sounds by cortical neurons. Nat Neurosci. 6:391–398.
Umbricht D, Vyssotki D, Latanov A, Nitsch R, Lipp HP. 2005. Deviance-related electrophysiological activity in mice: is there mismatch negativity in mice? Clin Neurophysiol. 116:353–363.
Velluti RA. 1997. Interactions between sleep and sensory physiology. J Sleep Res. 6:61–77.
von der Behrens W, Bauerle P, Kossl M, Gaese BH. 2009. Correlating stimulus-specific adaptation of cortical neurons and local field potentials in the awake rat. J Neurosci. 29:13837–13849.
Vyazovskiy VV, Cirelli C, Tononi G. 2011. Electrophysiological correlates of sleep homeostasis in freely behaving rats. Prog Brain Res. 193:17–38.
Vyazovskiy VV, Olcese U, Hanlon EC, Nir Y, Cirelli C, Tononi G. 2011. Local sleep in awake rats. Nature. 472:443–447.
Winkler I, Denham SL, Nelken I. 2009. Modeling the auditory scene: predictive regularity representations and perceptual objects. Trends Cogn Sci. 13:532–540.
Yamaguchi S, Globus H, Knight RT. 1993. P3-like potential in rats. Electroencephalogr Clin Neurophysiol. 88:151–154.
Zatorre RJ. 2007. There's more to auditory cortex than meets the ear. Hear Res. 229:24–30.